

Reaction of hydrogen sulfide with disulfide and sulfenic acid to form the strongly nucleophilic persulfide[†]

Ernesto Cuevasanta^{‡§}, Mike Lange[¶], Jenner Bonanata*, E. Laura Coitiño*, Gerardo Ferrer-Sueta^{**§}, Milos R. Filipovic^{¶1}, Beatriz Alvarez^{‡§2}

From the [‡]Laboratorio de Enzimología, *Laboratorio de Química Teórica y Computacional and ^{**}Laboratorio de Fisicoquímica Biológica, Facultad de Ciencias, and [§]Center for Free Radical and Biomedical Research, Universidad de la República, Montevideo, Uruguay; [¶]Department of Chemistry and Pharmacy, Division of Bioinorganic Chemistry, Friedrich-Alexander University of Erlangen–Nuremberg, Erlangen, Germany

Running title: *Reaction of H₂S with RSSR and RSOH to form RSSH*

¹To whom correspondence may be addressed: Milos R. Filipovic, Department of Chemistry and Pharmacy, Friedrich-Alexander University of Erlangen-Nuremberg, 91058 Erlangen, Germany; Tel: +49 91318527345; E-mail: milos.filipovic@fau.de.

²To whom correspondence may be addressed: Beatriz Alvarez, Laboratorio de Enzimología, Facultad de Ciencias, Universidad de la República, 11400 Montevideo, Uruguay; Tel: +598 25250749; E-mail: beatriz.alvarez@fcien.edu.uy.

Keywords: hydrogen sulfide; disulfide; sulfenic acid; hydrodisulfide; persulfide; thiol; kinetics

Background: Hydrogen sulfide (H₂S) modulates physiological processes in mammals.

Results: The reactivity of H₂S toward disulfides (RSSR) and albumin sulfenic acid (RSOH) to form persulfides (RSSH) was assessed.

Conclusion: H₂S is less reactive than thiols. Persulfides have enhanced nucleophilicity.

Significance: This kinetic study helps rationalize the contribution of the reactions with oxidized thiol derivatives to H₂S biology.

ABSTRACT

Hydrogen sulfide (H₂S) is increasingly recognized to modulate physiological processes in mammals through mechanisms that are currently under scrutiny. H₂S is not able to react with reduced thiols (RSH). However, H₂S – precisely, HS⁻ – is able to react with oxidized thiol derivatives. We performed a systematic study of the reactivity of HS⁻ toward symmetric low molecular weight disulfides (RSSR) and mixed albumin (HSA) disulfides. Correlations with thiol acidity and computational modeling showed that the reaction occurs through a concerted mechanism. Comparison to analogous reactions of thiolates indicated that the intrinsic reactivity of HS⁻ is one order of magnitude lower than that of thiolates. In addition, H₂S is able to react with sulfenic acids (RSOH). The rate constant of the reaction of H₂S with the sulfenic acid formed in

HSA was determined. Both reactions of H₂S with disulfides and sulfenic acids yield persulfides (RSSH), recently identified post-translational modifications. The formation of this derivative in HSA was determined and the rate constants of its reactions with a reporter disulfide and with peroxyxynitrite revealed that persulfides are better nucleophiles than thiols, consistent with the alpha effect. Experiments with cells in culture showed that treatment with hydrogen peroxide enhanced the formation of persulfides. Biological implications are discussed. Our results give light on the mechanisms of persulfide formation and provide quantitative evidence for the high nucleophilicity of these novel derivatives, setting the stage for understanding the contribution of the reactions of H₂S with oxidized thiol derivatives to H₂S effector processes.

INTRODUCTION

Beyond its classical conception as a highly toxic gas, hydrogen sulfide (H₂S)^a is now considered a physiological modulator in mammals. It is produced through the enzymatic activity of cystathionine β-synthase and cystathionine γ-lyase and probably also of mercaptopyruvate S-transferase (1). At neutral pH, the species H₂S, a weak acid (pK_a = 7 (2)), is in equilibrium with its conjugate base, the anion hydrosulfide (HS⁻). Simultaneously with the description of its

biological effects, efforts have been undertaken to elucidate the underlying molecular mechanisms, yielding slow progress. Hydrogen sulfide cannot react with thiols (RSH). Among a range of possible mechanisms that could operate in biological systems, the reaction of H₂S -more precisely, the hydrosulfide anion HS⁻ in equilibrium with it- toward disulfides (RSSR) and sulfenic acids (RSOH) can be considered a plausible way of unleashing physiological consequences. Furthermore, these reactions produce persulfides (also known as hydrodisulfides or hydropersulfides)^b, constituting possible mechanisms for the so-called 'S-sulfhydration' (3–5).

Persulfides (RSSH) represent novel thiol modification products of increasing interest in signaling and catalysis. They are constituent part of a class of chemical moieties known as sulfanes, in which sulfur is covalently linked to another sulfur and/or ionizable protons (6). The typically unstable persulfides possess electrophilic character. They also conserve the nucleophilic character of the original thiol, or actually increase it due to the presence of an adjacent sulfur containing unshared pairs of electrons -alpha effect- (3, 7, 8). Moreover, it has been proposed that these compounds are responsible for the biological effects initially assigned to H₂S (9). Persulfides were detected years ago as naturally occurring products (6) and proposed to have roles in sulfur transport (10) and enzymatic catalysis (11, 12). Indeed, animals have enzymes which produce and transfer persulfides, i.e. cystathionine γ -lyase, cystathionine β -synthase (13), sulfide:quinone oxidoreductase and rhodanese (14), and others which decompose them, like persulfide dioxygenase or ETHE1 (15). Recently, persulfides have been produced in a diversity of systems and detected using analytical methods such as cold cyanolysis and dithiothreitol-dependent release of H₂S, together with mass spectrometry and a variety of selective labeling methods (16–22).

Despite increasing efforts dedicated to understand the reactivity of H₂S, no systematic kinetic study of the reaction with oxidized thiol derivatives has been published and few persulfide models suitable for biochemical characterization have been proposed (17–19, 22). The reaction toward disulfides could represent a significant

consumption pathway for H₂S, mainly in extracellular milieu and plasma, where the diversity and high amounts of disulfides present (23) make them a likely target. In plasma, human serum albumin (HSA)^c is the most abundant protein and mixed disulfides of HSA constitute the predominant disulfides (23). HSA possesses 34 cysteines forming structural disulfides and only one reduced cysteine (Cys34, HSA-SH) that is located in a cleft, hindering intra and intermolecular reactions. These features allow a relatively stable sulfenic acid to be formed (HSA-SOH) (24). Sulfenic acids are transient intermediates generated in thiol oxidation pathways. They are typically unstable and decay mainly through reaction with a second thiol to form disulfides. Since HSA forms a long-lived and well characterized sulfenic acid (24, 25), it could open the way to kinetic measurements of the reactions with H₂S. In addition, HSA could potentially likewise form a stable persulfide (HSA-SSH).

In this work, we studied the reactivity of H₂S toward symmetrical low molecular weight (LMW) disulfides and mixed disulfides formed between HSA and LMW thiols, providing the first systematic study that allows comparison of the intrinsic reactivity of H₂S with respect to thiols. In addition, we report for the first time the rate constant of the reaction of H₂S with a sulfenic acid, the one formed in HSA. Last, we obtained the HSA persulfide and determined the rate constant of two of its reactions, providing the first quantitative analysis of the nucleophilicity of persulfides and its comparison to that of thiols. Thus, our study contributes to the understanding of the biochemical reactivity of H₂S and helps reveal the impact that its reactions with oxidized thiol derivatives to form hydrosulfides could have in the biology of this recently recognized mediator.

EXPERIMENTAL PROCEDURES

Preparation of hydrogen sulfide, LMW thiol and disulfide solutions. Stable Na₂S solutions were prepared by two methods: a) Stock solutions of Na₂S·9H₂O (J. T. Baker) were prepared daily in distilled water in sealed vials and used immediately. Concentrations were verified by iodometric titration and remained constant for several hours. b) Anhydrous Na₂S was purchased from Sigma Aldrich, opened and stored in a

glove box (< 1 ppm O₂ and < 1 ppm H₂O). Stock solutions (100 mM) were prepared in the glove box using argon-bubbled nano-pure water pretreated with Chelex resin-100 and stored in dark glass vials with PTFE septa at +4 °C. Gas-tight Hamilton syringes were used throughout the study. 5-Thio-2-nitrobenzoic acid (TNB) solutions were prepared as previously reported (26). LMW disulfides were purchased from Sigma or AppliChem. Glutathione disulfide (GSSG), cystinidimethylester (CysOMe-CysOMe) and hydroxyethyl disulfide (HED) stocks were prepared in distilled water; cystine (Cys-Cys) and homocystine (Hcy-Hcy) were diluted in NaOH 0.1 N; 5,5'-dithiobis-(2-nitrobenzoic acid) (DTNB) stocks were prepared in ethanol 95 %.

Preparation of HSA derivatives. HSA (Sigma) was delipidated, its thiol was reduced with β-mercaptoethanol and the concentration of protein and thiol were quantified as described previously (26). Mixed disulfides were prepared by incubating reduced HSA (~1 mM) overnight with the disulfide of interest (up to 20 mM) in acetate buffer (100 mM, pH 4.5, 0.1 mM diethylenetriaminepentaacetic acid (dtpa), 4 °C) or tris buffer (100 mM, pH 7.4, 0.1 mM dtpa, 4 °C). The pH of the buffer was chosen so as to favor maximum displacement of equilibria toward mixed disulfide formation: acidic pH when the pK_a of the leaving thiol was higher than that of HSA-SH (8.1, (23, 25)) as in the case of Hcy-Hcy, GSSG and HED, and basic pH when the pK_a was lower (DTNB, CysOMe-CysOMe) (27). The mixed disulfides were subjected to gel-filtration in a PD-10 column (GE) equilibrated with phosphate buffer (100 mM, pH 7.4, 0.1 mM dtpa) and the yield of disulfide was quantified by subtraction of HSA-SH concentration before and after treatment with LMW disulfides. HSA preparations enriched in sulfenic acid (HSA-SOH) were prepared by incubation of reduced HSA (0.6 mM) with H₂O₂ (4 mM, 4 min, 37 °C), kept on ice and used daily. The concentration of HSA-SOH was quantified by reaction with TNB (24). Sulfanes in HSA were produced following different procedures, depending on the experiment. For most determinations, mixed HSA disulfides were incubated with equimolar Na₂S in phosphate buffer (100 mM, pH 7.4, 0.1 mM dtpa, 25 °C) for a specified period, followed by gel-filtration. Persulfides for kinetic studies toward 4,4'-dithiodipyridine (DTDPy) were

prepared by incubating 6 μM HSA-SOH with equimolar Na₂S in phosphate buffer (100 mM, pH 7.4, 0.1 mM dtpa, 25 °C) during variable periods of time. Persulfides for kinetic studies toward peroxyxynitrite were prepared by reacting HSA-TNB with Na₂S. HSA-SSH was quantified based on the amount of TNB released and purified by gel-filtration on Sephadex G-10 equilibrated with phosphate buffer (30 mM, pH 7.4). Solutions were kept under argon and on ice to minimize decay.

Kinetics of hydrogen sulfide reactions with disulfides by continuous UV-Vis measurements. Reactions were initiated by the addition of low amounts (30-500 μM) of Na₂S to disulfides in pseudo-first order excess in borate (100 mM, pH 9.5, 0.1 mM dtpa) or phosphate (100 mM, pH 7.4, 0.1 mM dtpa) buffer using sealed quartz cuvettes with minimal head space. UV-Vis spectra were registered in a Varian Cary 50 spectrophotometer at 25 °C and increases in absorbance at 350 nm due to the appearance of sulfane sulfur (28) were fitted to single exponential functions in order to obtain pseudo-first order rate constants (*k*_{obs}) for Cys-Cys, CysOMe-CysOMe, GSSG, HED and Hcy-Hcy. The reaction with DTNB was followed from TNB formation at 412 nm and fitted to double exponential functions. The second-order rate constants were determined from the slopes of plots of *k*_{obs} versus disulfide concentration. The pH-independent rate constants were calculated by correction for HS⁻ taking into account the pH and the pK_a of H₂S.

Kinetics of hydrogen sulfide reactions with disulfides by discrete hydrogen sulfide measurements. Reaction mixtures containing excess disulfides in phosphate buffer (100 mM, pH 7.4, 0.1 mM dtpa) were incubated in closed vials with minimal head space at 25 °C. Aliquots were removed using a gas-tight syringe and mixed with 4 mM zinc acetate to quench the reaction. The H₂S concentration of the aliquots was determined using the methylene blue method (29). In the case of LMW disulfides, concentration decreases were fitted to single exponential functions to obtain the corresponding *k*_{obs}. In the case of mixed HSA disulfides, mixtures for methylene blue formation were centrifuged to remove the precipitated protein and the rate constants were calculated using the method of initial rates.

Kinetics of hydrogen sulfide reactions with disulfides by amperometric hydrogen sulfide measurements. Na₂S (10 μM) was injected into phosphate buffer (50 mM, pH 7.4) and its concentration was followed using a selective H₂S electrode connected to a Free Radical Analyzer (World Precision Instruments). The electrode response was continuously recorded. When it reached a maximum, different concentrations of HSA disulfides were injected. Decay of H₂S at 25 °C followed first order kinetics and the k_{obs} were plotted versus concentration of the protein derivative.

Kinetics of hydrogen sulfide reaction with the sulfenic acid in HSA using a competition approach. The reaction was evaluated through competition with TNB, using a procedure similar to a previously reported one (24). Sulfenic acid-enriched HSA (~ 0.5 μM HSA-SOH) was mixed with excess TNB (66 μM) in phosphate buffer (100 mM, pH 7.4, 0.1 mM dtpa) in the absence or presence of Na₂S (up to 100 μM). The decay of TNB was recorded at 412 nm and fitted to exponential plus straight line functions (24). The second-order rate constant for the reaction of H₂S with HSA-SOH was calculated from the slopes of plots of k_{obs} versus Na₂S concentration.

Sulfane quantification. The protein fraction was separated by gel-filtration and sulfane sulfur was quantified by cold cyanolysis. Samples were incubated with cyanide and the thiocyanate formed was determined by the absorbance of the complex formed with ferric ions at 460 nm (28).

Tag-switch assay. Labeling of persulfides in HSA preparations (dot-blots) and fixed cells was performed following an established protocol (19, 30). 2-(Methylsulfonyl)1,3-benzothiazole (MSBT) was purchased from Santa Cruz Biotechnology. CN-biotin was synthesized as previously (19, 30).

Detection of HSA persulfide with tris(2,4-dimethyl-5-sulfophenyl)phosphine (TDMSP). HSA-SSH (20 μM) was prepared from HSA-TNB by incubation with Na₂S at 1:1.5 molar ratio, purified on Sephadex G-10 and incubated with a 20-fold excess of TDMSP at room temperature for 30 min. The reaction mixture was sprayed into ultra-high resolution ESI-ToF Bruker Daltonik (Bremen, Germany) maXis5G, an ESI-ToF MS capable of resolution of at least

60,000 FWHM. Detection was performed in negative-ion mode and the source voltage was 4.0 kV. The flow rates were 180 μL/h. The instrument was calibrated by direct infusion of the Agilent ESI-TOF low concentration tuning mixture, which provided an m/z range of singly charged peaks up to 2700 Da in both ion modes.

Detection of HSA persulfide by ultra-high resolution ESI-ToF MS. HSA-TNB was mixed with equimolar Na₂S for 15 min at room temperature, desalted on Sephadex G10, mixed with acetonitrile (1/1, v/v) containing 0.5 % formic acid and continuously sprayed into maXis5G MS. Detection was performed in positive-ion mode and the source voltage was 4.5 kV. The flow rates were 180 μL/h. Spectra were post-processed using Data Analysis software (Bruker Daltonics).

Identification of the persulfidated Cys residue. HSA-SSH prepared from HSA-TNB was collected into vials containing 100 mM biotin-maleimide to ensure the immediate blocking of both, persulfides and eventually thiols. After 2 h incubation at 37 °C, the protein was desalted again on Sephadex G-10 and mixed with proteomics grade porcine trypsin (Sigma Aldrich, 1:100 w/w) overnight at 37 °C. The reaction was stopped by adjusting the pH to 3 and 100 μL of the peptide mixture was mixed with 100 μL Pierce™ Streptavidin Agarose beads (Thermo Fischer Scientific). The unbound peptides were discarded and the beads washed three times with phosphate buffer (50 mM, pH 7.4). The bound peptides were those modified by biotin-maleimide, but in the case of peptides initially containing persulfide, the reaction with biotin-maleimide creates a disulfide bond. These peptides were eluted by addition of 100 μL of 10 mM DTT. After centrifugation, the eluted peptides were analyzed by LC-MS. Reverse phase high-pressure liquid chromatography (Dionex, Thermo Fischer Scientific) was performed using a C18 column and a combination of water (solvent A) and acetonitrile (solvent B), both containing 0.5 % formic acid. The following elution protocol was used: 5 min of 10 % B and then 45 min of continuous rise to 90 % B. In addition, the peptides were directly injected into maXis5G using in-source collision-induced dissociation tandem MS approach (source voltage was 4.5 kV, source temperature 250 °C, collision energy 90 eV).

Reactivity of HSA persulfide toward peroxyxynitrite. Peroxyxynitrite was synthesized as described (31). Kinetic data were obtained by recording time-resolved UV–vis spectra using a modified μ SFM-20 Bio-Logic stopped-flow module equipped with a J&M TIDAS high-speed diode array spectrometer with combined deuterium and tungsten lamps (200–1015 nm wavelength range). The syringes were controlled by separate drives, allowing the variation of the ratio of mixing volumes used in the kinetic runs. Data were analyzed in the Specfit/32™ program. At least five kinetic runs were recorded for all conditions. Final concentration of peroxyxynitrite was 9 μ M and the concentrations of HSA-SSH and HSA-SH were in the range of 2–60 μ M. The yield of nitrotyrosine was determined by measuring absorbance at 430 nm ($\epsilon = 4400 \text{ M}^{-1} \text{ cm}^{-1}$) after alkalization to pH 10, 5 min after mixing 183 μ M protein with 500 μ M peroxyxynitrite in phosphate buffer (50 mM, pH 7.4).

Reactivity of HSA persulfide toward DTDPy. An Applied Photophysics RX2000 stopped-flow accessory coupled to a Varian 50 spectrophotometer was used. Preparations enriched in HSA-SOH were incubated with equimolar Na_2S in one syringe and mixed at increasing time points with excess DTDPy contained in the other syringe, in phosphate buffer (100 mM, pH 7.4, 0.1 mM dtpa) at 25 °C. The time course of thiopyridone appearance was followed at 324 nm ($\epsilon = 21400 \text{ M}^{-1} \text{ cm}^{-1}$). The traces were fitted to double exponential functions to obtain the corresponding k_{obs} .

Computational modeling of the reaction mechanism of HS^- with a representative symmetrical LMW disulfide (zwitterionic Cys-Cys) in aqueous solution. The structures of the reactant and product complexes and the corresponding transition state including two explicit water molecules were fully optimized and verified by inspection of the eigenvalues of the Hessian matrix at the IEFPCM/ ω B97X-D/6-31+G(d) (32–34) level of theory, as implemented in Gaussian09 rev. D.01 (35). Water was also described as a continuum solvent ($\epsilon = 78.5$), placing solutes in molecular-shaped cavities constructed using Bondi's radii (36). The reaction path was followed by the intrinsic reaction coordinate (37) calculated at the same level of theory with the Hessian-based Predictor-

Corrector integrator algorithm (38), 50 points each side of the transition state with a step size of 0.05 Bohr. Thermochemistry at 298 K and 1 atm was assessed at the same level of theory, applying usual approximations of statistical thermodynamics and unscaled zero point vibrational energies, as implemented in the Gaussian09 suite (35).

Computational comparison of the global reactivity and nucleophilicity of HS^- and Cys persulfide with respect to LMW thiolates. The structures of five LMW thiolates of known basicity (cysteinemethylester, CysOMe; cysteinylglycine, Cys-Gly; cysteine, Cys; β -mercaptoethanol, β -ME; homocysteine, Hcy) as well as cysteine persulfide anion (CysSS^-) were determined at the same level of theory in aqueous solution as described above. The energy of the highest occupied Kohn-Sham (KS) orbital, E_{HOMO} , was taken as an indicator of the nucleophilicity of each species. The corresponding global reactivity was quantified by the chemical hardness (η), calculated under the finite differences approximation with the following equation (39):

$$\eta = (E_{\text{LUMO}} - E_{\text{HOMO}})/2 \quad (\text{Eq. 1})$$

where E_{LUMO} represents the energy of the lowest unoccupied KS orbital.

Computational prediction of the pK_a of cysteine persulfide. Using the same level of theory described above, a prediction of the pK_a shift (ΔpK_a) corresponding to CysSSH with respect to CysSH was obtained by applying the proton-exchange method proposed by Yu *et al.* (40) with the calculated free-energy, ΔG_{exch} , corresponding to the reaction:



from which ΔpK_a is obtained as follows:

$$\Delta\text{pK}_a = \Delta G_{\text{exch}}/(2.303 \text{ RT}) \quad (\text{Eq. 3})$$

Cell experiments. Human umbilical vein endothelial cells (HUVEC) (PromoCell) were grown in endothelial cell growth medium 2 (ready-to-use, PromoCell) on ibidi dishes (ibidi, Martinsried, Germany) at 5 % CO_2 and 20 % oxygen until they reached > 50 % confluency. Human neuroblastoma cells (SH-SY5Y, ECACC, Sigma Aldrich) were grown in Ham's

F12:EMEM (EBSS) (1:1) medium supplemented with 2 mM glutamine, 1 % non-essential amino acids + 15 % fetal bovine serum FBS / FCS, on ibidi dishes. Inhibition of endogenous production of H₂S was performed by using oxamic acid (2 mM) in SH-SY5Y cultures or propargylglycine (2 mM) in HUVEC cultures. Fluorescence microscopy was carried out using Carl Zeiss Axiovert 40 CLF inverted microscope, equipped with green fluorescent filters and AxioCam ICm1. Images were post processed in ImageJ software.

Data processing. Data were processed using OriginPro 8 (Microcal Software). Numerical fitting of data to reaction sequences was performed with Gepasi (41).

RESULTS AND DISCUSSION

Kinetics of reaction of hydrogen sulfide with symmetric LMW disulfides. In order to evaluate the reaction of H₂S toward LMW disulfides, kinetic measurements were performed. Parallel approaches were used in most cases. Under pseudo-first order conditions with disulfides in excess, exponential decays in H₂S concentration were observed (Fig. 1A). The reactions are likely to reach equilibrium situations, but under our conditions the consumption of H₂S was close to total, probably because of the excess disulfide reagent and because of further reactions of the products. The observed rate constants showed a linear dependence on disulfide concentration (Fig. 1B). The second-order rate constants for six disulfides are summarized in Table 1. The values were in the order of 10⁻² to 10⁰ M⁻¹ s⁻¹ for alkyl disulfides. Since HS⁻ is the species responsible for reactivity, the rate constants determined at pH 7.4 were corrected to obtain the pH-independent values, which represent the rate constants that would be measured if all the H₂S was ionized to HS⁻. Results obtained by initial rate processing or by UV-Vis absorbance measurements were consistent with H₂S consumption measurements.

As precedent, rate constants of (6.2 ± 0.7) × 10⁻² and 1.3 × 10⁻² M⁻¹ s⁻¹ have been reported for the reaction of cystine with excess H₂S in 50 mM borate buffer at pH 10.0 or NaOH 0.1 M, respectively (42). These values are lower, by factors of 15-70, than the pH-independent rate constant determined in this work, (9 ± 2) × 10⁻¹ M⁻¹ s⁻¹. The difference can be explained because

at alkaline pHs the predominant species is cystine²⁻ and not the zwitterion, as in our conditions. In addition, HS⁻ may ionize to S²⁻. A change in the charge in the reacting species could affect the reaction rate constant by two orders of magnitude (43). Recently, Vasas et al (44) kinetically characterized the reaction of H₂S with DTNB. The second-order rate constant reported at pH 7.4 is 881 M⁻¹ s⁻¹, consistent with our determination (861 M⁻¹ s⁻¹, Table 1). They also report that the kinetics of reaction with cysteine and glutathione are significantly slower.

Kinetics of reaction of hydrogen sulfide toward asymmetric disulfides of HSA formed with LMW thiols. Second-order rate constant were obtained for the reactions of H₂S with several mixed disulfides (Table 2) by measuring initial rates of H₂S consumption using the methylene blue method (Fig. 2A). The values were in the order of 10⁻¹-10¹ M⁻¹ s⁻¹ for the disulfides formed between HSA and alkyl thiols. Controls were performed using HSA-SH to rule out the reduction of structural disulfides as well as other decay pathways of H₂S such as autooxidation. Rate constants were also determined by following the disappearance of H₂S amperometrically, with similar results (Fig. 2B).

Mechanism of the reaction of hydrogen sulfide toward disulfides. The data obtained for H₂S can be rationalized in the context of reported data for thiol-disulfide interchange reactions. These interchange reactions occur by single concerted S_N2 mechanisms where the reactive species involved is the thiolate anion (45). When the pH-independent rate constants are plotted against the pK_as of a variety of attacking thiols and target disulfides, Brønsted correlations are obtained according to the following equation:

$$\log k = \beta_{\text{nuc}} \text{p}K_{\text{a}}^{\text{nuc}} + \beta_{\text{c}} \text{p}K_{\text{a}}^{\text{c}} + \beta_{\text{lg}} \text{p}K_{\text{a}}^{\text{lg}} + C \quad (\text{Eq. 4})$$

where β_{nuc}, β_c, β_{lg} are the Brønsted coefficients for the nucleophilic sulfur, central sulfur and leaving group sulfur, respectively. Analogously, for the reaction studied herein of HS⁻ with symmetrical disulfides producing a thiolate (leaving group) and a persulfide, the logarithm of the pH-independent rate constants obtained show a negative linear correlation with the pK_a of the leaving thiol (Fig. 3A), supporting a simple concerted S_N2 mechanism and indicating that acidic thiols -with lower pK_as- are better leaving

groups. The slope of this curve represents the addition of the Brønsted coefficients of central and leaving sulfurs ($\beta_c + \beta_{lg}$) and has a value of -0.75, consistent with the values reported for the reaction with thiolates (45). In the case of mixed disulfides of HSA and LMW thiols, the slope of the Brønsted plot was -0.6, reflecting β_c or β_{lg} (Fig. 3B). The leaving group can be either HSA-S⁻ or RS⁻. In the absence of steric effects, the most acidic groups will be the preferred leaving groups.

Computational modeling. The structures of the reactant complex, transition state and product complex for the reaction mechanism of HS⁻ with cystine -as a representative LMW disulfide- are shown in Fig. 4. The reaction exhibits a concerted linear transition state (with an associated imaginary frequency of $233i\text{ cm}^{-1}$) consistent with a typical S_N2 mechanism. The explicit water molecules present in the model are not directly involved in the reaction coordinate but play an ancillary role stabilizing the participant moieties through hydrogen bonding. The Gibbs free-energy of reaction is predicted to be of $13.4\text{ kcal mol}^{-1}$. Although formation of the products would thus appear to be thermodynamically disfavored, fast acid base equilibration of the products is expected to drive the outcome of the process. Precisely, since CysSH has a pK_a of 8.29 and the predicted pK_a for CysSSH as obtained from Eq. 3 is 4.34 (ΔpK_a of -3.96, Table 3), the products at physiological pH become CysSS⁻ and CysSH, preventing the reverse reaction. The activation Gibbs free-energy is calculated to be of $19.9\text{ kcal mol}^{-1}$. This value is comparable to the experimental one of $17.5\text{ kcal mol}^{-1}$ that can be derived from the rate constant by applying the Eyring-Polanyi equation, confirming the consistency between theory and experiment in the description of the reaction.

Comparison of nucleophilicities of hydrosulfide and thiolates. The pH-independent rate constants obtained for HS⁻ reactions with the six symmetric disulfides studied are about one order of magnitude lower than those reported for alkyl thiolates of comparable pK_a (Fig. 3A). This decreased nucleophilic character of HS⁻ could be due to the lack of the inductive effect of the adjacent methylene of the sulfur, changes in the polarizability of the sulfur or solvation effects (8, 46).

The effect of the pK_a of the nucleophile on the reaction with a disulfide is evident from Fig. 5, where the pH-independent rate constants of thiol disulfide interchange reactions for different thiolates with DTNB or GSSG, taken from the literature (45, 47), are compared with the value obtained for HS⁻. Again, the intrinsic reactivity of HS⁻ is lower than that of thiolates, by factors of 20-25.

Although the intrinsic reactivity of HS⁻ is lower than that of thiolates, at pH 7.4 its availability is higher. Indeed, the ratio HS⁻/H₂S is 2.51 at pH 7.4 due to the low pK_a of H₂S, while the ratio thiolate/thiol for cysteine and glutathione are 0.13 and 0.03, respectively. The Brønsted correlation can be used to obtain a theoretical optimum pK_a for maximizing the observed rate for reactions at a certain pH (43).

$$(1-\beta_{\text{nuc}})/\beta_{\text{nuc}} = 10^{(\text{pH}-\text{p}K_a)} \quad (\text{Eq. 5})$$

Considering a β_{nuc} value of 0.38 (Fig. 5A), the optimal pK_a for the reaction at pH 7.4 is 7.2. This means that at physiological pH the nucleophilic capacity of H₂S is maximally exploited. In other words, although H₂S is a relatively weak nucleophile, its reactivity is maximized at physiological pHs.

As shown by inspection of the calculated descriptors of global reactivity and nucleophilicity collected in Table 3, HS⁻ is harder and a weaker nucleophile than the thiolates. The nucleophilicities (estimated through the KS-HOMO energies, E_{HOMO}, as a measure of the facility of each species to donate electrons) of the five thiolates linearly correlate with the corresponding experimental pK_a (Fig. 6) mirroring the trend emerging from the experimental data and showing that more basic thiolates are better nucleophiles (Fig. 5). In contrast, the nucleophilicity of HS⁻ falls below that of a thiolate of comparable basicity.

Detection of HSA persulfide. The formation of a persulfide in HSA could not only represent a potential physiological product, but could also be a useful model to study its features, as in the example of sulfenic acids (26). Using the method of cold cyanolysis, the formation of sulfane sulfur, a group of compounds that includes persulfide, was evaluated. Sulfane sulfur was detected in reaction mixtures of asymmetric HSA

disulfides with Na₂S and coeluted with protein in gel-filtration separations (Fig. 7A).

In addition, a selective method for persulfide detection has been recently developed, the tag-switch assay, which labels protein persulfides with biotin (19, 30). HSA-SSH formed through the reaction of several mixed disulfides with Na₂S were analyzed for the level of biotin labeling by dot-blot assay to confirm that indeed, in all tested cases, HSA-SSH is formed (Fig. 7B). Control experiments performed with the mixed disulfides in the absence of Na₂S gave negative results, with the only exception of HSA-TNB that showed a weak signal (data not shown).

Sulfane sulfur reacts with triphenylphosphine and its derivatives to give the corresponding sulfide. This reaction has been recently used as a basis for a new method for sulfane sulfur quantification (48). We used a water soluble phosphine, TDMSP, to prove HSA-SSH formation. HSA-SSH prepared from HSA-TNB incubation with Na₂S was treated with TDMSP and analyzed by negative-ion mode ultra-high resolution ESI-TOF MS. The spectrum of the reaction mixture (Figs. 8A and B, for two different *m/z* ranges) suggested formation of TDMSP sulfide (TDMSP=S). Namely, although the strongest signals were assigned to unreacted TDMSP, flying as [TDMSP + Na]²⁻ (Fig. 8C) and [TDMSP + 2Na] (Fig. 8D), the presence of TDMSP=S with one sodium (Fig. 8E) or two sodium cations (Fig. 8F) was also observed. The peak intensity was ~4.5 % matching nicely the assumed TDMSP/persulfide ratio.

HSA-SSH was also analyzed by MS before and after the equimolar addition of Na₂S to HSA-TNB. An obvious shift toward lower *m/z* could be observed in the sample of HSA-TNB treated with H₂S (Figs. 9A and 9B) suggesting the loss of the TNB moiety. Spectral deconvolution confirmed this as shown in Fig 9C. The appearance of a new peak corresponded well to the loss of the TNB moiety and the addition of sulfur, i.e. formation of HSA-SSH. In addition, a mass change consistent with the formation of HSA-SSO₃⁻ was observed, in accordance with previous observations on bovine serum albumin and glutathione peroxidase (18, 19). The mass of the protein was higher than expected, probably because of the presence of sodium ions.

Nevertheless, the mass differences are in agreement with the changes expected.

Finally, we also proved that the actual site of HSA persulfidation is Cys34 (Figs. 9D, 9E and 9F). To do so we designed an approach, adapted from (5), in which HSA-SSH, generated in the reaction between HSA-TNB and H₂S, was mixed with biotin-maleimide. This alkylated free thiols and also reacted with persulfides forming a mixed disulfide. Protein was then trypsinized and streptavidin beads added into the peptide mixture. Only labeled peptides are expected to bind to the streptavidin beads. After careful washout, the peptide which originally contained persulfide was eluted with DTT, which reduces the mixed disulfide formed in the reaction with biotin-maleimide (Fig. 9D). The peptide was then analyzed by HPLC-MS. The positive-ion mode analysis revealed the presence of the Cys34 peptide ALVLIAFAQYLQQCPFEDHVK as the doubly charged species (Fig 9E). Subsequent collision-induced dissociation analysis further confirmed it (Fig. 9F).

Kinetics of reaction of hydrogen sulfide with the sulfenic acid of HSA. The reaction of H₂S toward sulfenic acid provides an alternative way to form persulfide. To kinetically evaluate this reaction in HSA, an experimental design involving competition between H₂S and TNB for HSA-SOH was used. The *k*_{obs} of TNB consumption increased and the amplitude decreased with Na₂S concentration (Figs. 10A and 10B). From the slope obtained (Eq. 6), we could calculate a rate constant of (2.7 ± 0.8) × 10² M⁻¹ s⁻¹ for the reaction of H₂S with HSA-SOH at pH 7.4 and a pH-independent rate constant of (4 ± 1) × 10² M⁻¹ s⁻¹ (assuming that all HSA-SOH was protonated).

$$k_{\text{obs}} = k_{\text{TNB}} [\text{TNB}] + k_{\text{H}_2\text{S}} [\text{H}_2\text{S}] \quad (\text{Eq. 6})$$

This is to our knowledge the first kinetic report regarding the reactivity of H₂S toward a sulfenic acid. In contrast to the trend observed for LMW disulfides (Figs 3 and 5), the pH-independent rate constant of HS⁻ reaction with HSA-SOH is higher than those of Cys, GSH and TNB (1.1, 1.0 and 1.9 × 10² M⁻¹ s⁻¹, respectively, (24) and similar to Hcy (4.8 × 10² M⁻¹ s⁻¹), which p*K*_a is two units higher. This difference can be explained by steric hindrance, since Cys34 is partially buried in the protein surface and HS⁻ could have easier access than thiolates.

Reactivity of hydrogen sulfide toward disulfides and sulfenic acids in cellular context. Oxidized thiols that could constitute molecular targets for H₂S (i.e. disulfides and sulfenic acids) are scarce in the cytoplasmic environment. Accordingly, the majority of protein persulfides has been found to be located in the endoplasmic reticulum, an organelle rich in protein oxidized thiols (19). The influence of oxidative conditions could increase the probability of inducing the formation of persulfides in cells. We addressed this possibility by treating cells in culture with H₂O₂, with or without the prior inhibition of the intracellular production of H₂S. We used the tag-switch assay to detect persulfide levels in HUVEC and SH-SY5Y cells (Fig. 11). In both cell lines the treatment with H₂O₂ led to a significant increase in the total persulfide levels as evidenced by fluorescence microscopy. More importantly, we assessed the effect of the inhibition of the endogenous production of H₂S. For HUVEC, propargylglycine was used, a relatively specific inhibitor of cystathionine γ -lyase. For SH-SY5Y cells, oxamic acid was used, which inhibits both cystathionine β -synthase and cystathionine γ -lyase, as shown recently (49). Inhibition of endogenous H₂S production abolished H₂O₂-induced effects suggesting that the reaction of H₂S with oxidized thiols could be an important source of endogenous persulfides (Fig. 11).

Kinetics of reaction of the persulfide of HSA toward electrophiles. Both, reactions of H₂S with disulfides and with sulfenic acids yield persulfides. These products are likely to have enhanced nucleophilic reactivity with respect to thiolates. Several publications suggest that persulfides are better nucleophiles than thiols, but so far there are no quantitative kinetic analysis reported (13, 17).

We first studied the reactivity of HSA-SSH toward peroxyxynitrite (ONOO⁻/ONOOH), the product of the reaction of nitric oxide and superoxide radicals. For these experiments, the persulfide concentration was judged based on the yield of TNB released from HSA-TNB after it reacted with Na₂S and prior to desalting. An initial rate approach was used to analyze the kinetic traces obtained (50), since a pseudo-first order excess of HSA-SSH could not be reached. The initial rate increased linearly with the assumed concentration of HSA-SSH, leading to a rate constant of $(1.2 \pm 0.4) \times 10^4 \text{ M}^{-1} \text{ s}^{-1}$ at 20 °C

(Fig. 12). This value is likely an underestimation due to HSA-SSH instability and to the difficulty in exactly knowing its concentration. For comparison, HSA-SH reacted more slowly with peroxyxynitrite, $(2.7 \pm 0.3) \times 10^3 \text{ M}^{-1} \text{ s}^{-1}$, under the same conditions, confirming the higher reactivity of the persulfide with respect to the thiol. It is worth mentioning that along with the increased kinetics for the reaction with peroxyxynitrite, we observed decreased nitrotyrosine levels (0.041 vs 0.071 moles nitrotyrosine/mol protein for HSA-SSH vs HSA-SH, respectively).

In order to improve the quantitative assessment of the nucleophilicity of HSA-SSH, we then evaluated its reactivity toward DTDPy. The use of the disulfide DTDPy as target presents advantages: it has high intrinsic reactivity, the reaction can be followed through thiopyridone absorbance, and it can be used in pseudo first-order excess, eliminating the need for accurately knowing the concentration of the persulfide. When equimolar amounts of HSA-SOH and Na₂S were incubated for a certain time and aliquots mixed with excess DTDPy in a stopped-flow device, an initial fast increment in thiopyridone absorbance was detected (Fig. 13A). Controls using HSA-SH and HSA-SOH preparations in the absence of H₂S also showed an absorbance increase but lacked the first fast phase. For the latter, the absorbance increase likely represented remnant thiols. The observed rate constants were linearly dependent on DTDPy concentration, and a second-order rate constant of $(1.7 \pm 0.1) \times 10^4 \text{ M}^{-1} \text{ s}^{-1}$ for HSA-SSH was determined (pH 7.4, 25 °C), higher than those observed for HSA-SH or HSA-SOH preparations: $(7.6 \pm 0.4) \times 10^2 \text{ M}^{-1} \text{ s}^{-1}$ and $(6.4 \pm 0.1) \times 10^2 \text{ M}^{-1} \text{ s}^{-1}$, respectively (Fig. 13B). In addition, an increase in the amplitude of the initial fast phase with time was observed, indicative of the time course of HSA-SSH formation (Figs. 13C-D). The rate constant of the reaction between HSA-SOH and H₂S was estimated from the fit of the amplitude versus incubation time plot using a Levenberg-Marquardt algorithm included in Gepasi, considering also the spontaneous decay of HSA-SOH ($5.6 \times 10^{-4} \text{ s}^{-1}$ at 25 °C (23)) (Fig. 13D). A value of $(4.7 \pm 0.2) \times 10^2 \text{ M}^{-1} \text{ s}^{-1}$ was obtained, consistent with that determined by competition with TNB.

The evaluation of nucleophilicity by means of DTDPy demonstrates twenty-fold increased reactivity of the persulfide at pH 7.4 in comparison to thiol. The pK_a of HSA-SSH is likely to be several units lower than the original HSA-SH (Table 3) resulting in an estimated pH-independent rate constant close to the value determined at pH 7.4, $\sim 2 \times 10^4 \text{ M}^{-1} \text{ s}^{-1}$. On the other hand, the pH-independent rate constant for HSA-SH can be calculated considering the pK_a of 8.1, as $\sim 7 \times 10^3 \text{ M}^{-1} \text{ s}^{-1}$. This value is lower than that determined for HSA-SSH by a factor of ~ 3 . The enhanced reactivity of a nucleophilic atom when it is adjacent to an atom containing one or more unshared pairs of electrons is a classic observation, referred to as the alpha effect (7, 8). For another reaction, that of different nucleophiles with the ester *p*-nitrophenyl acetate, the alpha effect is associated with increases in reactivity by factors of 10-100 (7, 51). By comparison, the extent of the effect in our case is more modest. The higher reactivity of HSA-SSH with respect to HSA-SH is consistent with the computational calculations performed for cysteine persulfide, that show a higher intrinsic nucleophilicity than the corresponding thiol (increased KS-HOMO energy) as well as decreased chemical hardness (Table 3 and Fig. 6). The latter could confer preferential reactivity toward soft electrophiles such as heavy metal cations (52), alkyl halides and Michael electrophiles (18). Our study is, to our knowledge, the first evaluation of the magnitude of the alpha effect for a persulfide.

Biological implications. Consistent with the limited intrinsic nucleophilicity of H_2S , the rate constants of the reactions with LMW and HSA disulfides are relatively low. In order to extrapolate how these reactions could contribute to H_2S decay, factors of rate constant times concentration together with competing pathways and compartmentalization aspects need to be taken into account.

In the intravascular space, a compartment where disulfides are abundant, factors of rate constant times concentration can be evaluated considering the total concentration levels of LMW and HSA disulfides ($\sim 250 \mu\text{M}$ (23)) and the rate constants now known (Tables 1 and 2). Thus, a global half-life of 26 min can be estimated for this process in plasma. However, from previous work (53, 54) it is known that H_2S can traverse membranes easily

and that methemoglobin in red blood cells can participate in its clearance. Recently, consumption rates for H_2S by methemoglobin consistent with a half-life of 4 min in blood were reported (55). This value is within one order of magnitude of that ascribed to disulfides. Thus, variations in the levels of methemoglobin or disulfides could produce changes in the relative contributions of disulfides and red blood cells to H_2S decay rate.

Targets in the extravascular milieu can also be involved in H_2S clearance. The high permeability of membranes allows mitochondria to become a sink for H_2S , limiting its half-life in the cell. Formation of persulfides by direct reaction of H_2S with disulfides and sulfenic acids is probably under kinetic competition with mitochondrial consumption. In this regard, an interesting scenario could be set in the nervous system, where H_2S scavenging by mitochondria is inefficient due to the lack of sulfide:quinone oxidoreductase activity (56), the enzyme responsible for the first step of the mitochondrial catabolism of H_2S , and effects of endogenous H_2S on non-mitochondrial persulfide generation are probably maximized.

In the cytoplasmic environment, the reaction of H_2S with LMW and typical protein disulfides or sulfenic acids is kinetically challenged due to the low concentration of oxidized thiols and the relatively low rate constants, in the context of high concentrations of reduced thiols that might compete with H_2S . Thus, situations that lead to increased steady state levels of oxidized thiols increase persulfide formation. Based in our experiments with cells in culture treated with H_2O_2 , the reaction of H_2S with oxidized thiols is a plausible pathway for persulfide production in cytoplasmic and reticulum environments in response to oxidative signals. In addition to the direct reaction of H_2S with oxidized thiols, alternative pathways for persulfide formation *in vivo* can involve the consumption of cystine by cystathionine β -synthase or cystathionine γ -lyase (13). Furthermore, proteins that participate in H_2S oxidation pathways can generate intermediate persulfides that can subsequently be transferred to other targets (57).

It is important to bear in mind that the rate constants of H_2S reactions can be accelerated in the case of particular protein contexts. Proof of

concept for the potential acceleration of the reaction of H₂S with a disulfide by the protein environment is provided by sulfide:quinone oxidoreductase. This flavoprotein catalyzes the oxidation of H₂S to sulfane sulfur at the expense of ubiquinone. The process starts with the reaction of H₂S with a critical protein disulfide, and values of $k_{cat}/K_{M,sulfide}$ of $10^7 \text{ M}^{-1} \text{ s}^{-1}$ (58, 59) demonstrate an extraordinary acceleration with respect to free cystine ($0.6 \text{ M}^{-1} \text{ s}^{-1}$). Likewise, wide variations in rate constants are expected for the reactions of H₂S with different protein sulfenic acids. To achieve specificity, one aspect that H₂S could invoke, as suggested by the case of HSA-SOH, is a steric advantage for reaction with constrained disulfides and sulfenic acids due to its small size in comparison to other cellular nucleophiles. In fact, from the point of view of biological function, the low rate constants of the uncatalyzed processes constitute actually an asset, opening the way to kinetic control.

Persulfides are promising candidates to constitute intermediate species in the modulation of cellular functions by H₂S. The levels of persulfides are so far hard to evaluate in biological samples due to the instability of these compounds and to the lack of rapid and selective analytical methods, which are still under development. Persulfides have been proposed to protect the original thiol from irreversible oxidative modifications (60). They have been reported to participate in the synthesis of sulfur-containing molecules (11) and to be involved in enzymatic catalysis and regulation (6). The twenty-fold increased reactivity of the HSA persulfide relative to the HSA thiol at pH 7.4 underscores the improved nucleophilicity of these derivatives with respect to the parent thiol and to H₂S. As functions for persulfides in biological systems continue to be unraveled, this increased nucleophilicity is likely to play a key role in explaining the underlying molecular mechanisms.

CONCLUSIONS

Our study reveals several aspects relative to the reactivity of H₂S, summarized as follows:

- Hydrogen sulfide reacts with LMW and mixed protein disulfides to produce persulfides.
- The reaction occurs through a concerted mechanism, similar to the thiol-disulfide interchange reaction.

- The intrinsic reactivity observed for HS⁻ toward disulfides is lower than that reported for thiolates, probably due to the absence of the inductive effect of the methylene adjacent to the sulfur atom, increased chemical hardness or solvation.
- Hydrogen sulfide is able to react with the sulfenic acid in HSA, proving another pathway for persulfide formation.
- Experiments with cells in culture indicate that persulfide formation increases upon exposure to H₂O₂, consistent with the proposed processes.
- Kinetic determinations evidence that the persulfide has increased nucleophilic reactivity than the parent thiol, as expected from the alpha effect.

Overall, our study sets the stage for understanding the reactivity of H₂S toward oxidized thiol derivatives and the possible contribution of persulfides to the biological effects of this novel endogenous modulator.

ACKNOWLEDGMENTS

We thank Matías N. Möller, Laura Antmann, Lucía Turell, Martina Steglich (Universidad de la República, Uruguay) and Jan Miljkovic (University of Erlangen–Nuremberg, Germany) for helpful discussions and technical assistance. The authors are grateful to professor Ivana Ivanovic-Burmazovic (FAU) for the use of the equipment.

CONFLICT OF INTEREST

The authors declare that they have no conflicts of interest with the contents of this article.

AUTHOR CONTRIBUTIONS

E.C. designed, performed and analyzed experiments and wrote the manuscript. J.B. and E.L.C. designed, performed and analyzed the computational experiments, and wrote the corresponding parts. G.F.S. helped design and analyze experiments and edited the manuscript. M.R.F. designed, performed and analyzed mass spectrometry, tag-switch, amperometric kinetics, peroxyxynitrite and cell experiments with the assistance of M.L., and co-wrote the manuscript. B.A. conceived, designed and analyzed experiments and wrote the manuscript. All authors approved the final version.

REFERENCES

1. Kabil, O., and Banerjee, R. (2010) Redox biochemistry of hydrogen sulfide. *J. Biol. Chem.* **285**, 21903–7
2. Cotton, F., and Wilkinson, G. (1988) *Advanced Inorganic Chemistry*, New York
3. Paulsen, C. E., and Carroll, K. S. (2013) Cysteine-mediated redox signaling: chemistry, biology, and tools for discovery. *Chem. Rev.* **113**, 4633–4679
4. Mustafa, A. K., Gadalla, M. M., Sen, N., Kim, S., Mu, W., Gazi, S. K., Barrow, R. K., Yang, G., Wang, R., and Snyder, S. H. (2009) H₂S signals through protein S-sulfhydration. *Sci. Signal.* **2**, ra72
5. Sen, N., Paul, B. D., Gadalla, M. M., Mustafa, A. K., Sen, T., Xu, R., Kim, S., and Snyder, S. H. (2012) Hydrogen sulfide-linked sulfhydration of NF- κ B mediates its antiapoptotic actions. *Mol. Cell.* **45**, 13–24
6. Toohey, J. I. (1989) Sulphane sulphur in biological systems: a possible regulatory role. *Biochem. J.* **264**, 625–632
7. Jencks, W. P., and Carriuolo, J. (1960) Reactivity of nucleophilic reagents toward esters. *J. Am. Chem. Soc.* **82**, 1778–1786
8. Edwards, J. O., and Pearson, R. G. (1962) The factors determining nucleophilic reactivities. *J. Am. Chem. Soc.* **84**, 16–24
9. Toohey, J. I. (2011) Sulfur signaling: is the agent sulfide or sulfane? *Anal. Biochem.* **413**, 1–7
10. Olson, K. R. (2009) Is hydrogen sulfide a circulating “gasotransmitter” in vertebrate blood? *Biochim. Biophys. Acta.* **1787**, 856–863
11. Wright, C. M., Christman, G. D., Snellinger, A. M., Johnston, M. V., and Mueller, E. G. (2006) Direct evidence for enzyme persulfide and disulfide intermediates during 4-thiouridine biosynthesis. *Chem. Commun. (Camb.)* (29), 3104–310610
12. Mueller, E. G. (2006) Trafficking in persulfides: delivering sulfur in biosynthetic pathways. *Nat. Chem. Biol.* **2**, 185–194
13. Ida, T., Sawa, T., Ihara, H., Tsuchiya, Y., Watanabe, Y., Kumagai, Y., Suematsu, M., Motohashi, H., Fujii, S., Matsunaga, T., Yamamoto, M., Ono, K., Devarie-Baez, N. O., Xian, M., Fukuto, J. M., and Akaike, T. (2014) Reactive cysteine persulfides and S-polythiolation regulate oxidative stress and redox signaling. *Proc. Natl. Acad. Sci. U.S.A.* **111**, 7606–7611
14. Hildebrandt, T. M., and Grieshaber, M. K. (2008) Three enzymatic activities catalyze the oxidation of sulfide to thiosulfate in mammalian and invertebrate mitochondria. *Febs J.* **275**, 3352–61
15. Kabil, O., and Banerjee, R. (2012) Characterization of patient mutations in human persulfide dioxygenase (ETHE1) involved in H₂S catabolism. *J. Biol. Chem.* **287**, 44561–44567
16. Ubuka, T. (2002) Assay methods and biological roles of labile sulfur in animal tissues. *J. Chromatogr. B Analyt. Technol. Biomed. Life Sci.* **781**, 227–49
17. Francoleon, N. E., Carrington, S. J., and Fukuto, J. M. (2011) The reaction of H₂S with oxidized thiols: generation of persulfides and implications to H₂S biology. *Arch. Biochem. Biophys.* **516**, 146–153
18. Pan, J., and Carroll, K. S. (2013) Persulfide reactivity in the detection of protein S-sulfhydration. *ACS Chem. Biol.* **8**, 1110–1106
19. Zhang, D., Macinkovic, I., Devarie-Baez, N. O., Pan, J., Park, C.-M., Carroll, K. S., Filipovic, M. R., and Xian, M. (2014) Detection of protein S-sulfhydration by a tag-switch technique. *Angew. Chem. Int. Ed. Engl.* **53**, 575–581
20. Nagahara, N., Nirasawa, T., Yoshii, T., and Niimura, Y. (2012) Is novel signal transducer sulfur oxide involved in the redox cycle of persulfide at the catalytic site cysteine in a stable reaction intermediate of mercaptopyruvate sulfurtransferase? *Antioxid. Redox Signal.* **16**, 747–753
21. Chatterji, T., Keerthi, K., and Gates, K. S. (2005) Generation of reactive oxygen species by a persulfide (BnSSH). *Bioorg. Med. Chem. Lett.* **15**, 3921–3924
22. Bailey, T. S., Zakharov, L. N., and Pluth, M. D. (2014) Understanding hydrogen sulfide storage: probing conditions for sulfide release from hydrodisulfides. *J. Am. Chem. Soc.* **136**, 10573–10576

23. Turell, L., Radi, R., and Alvarez, B. (2013) The thiol pool in human plasma: the central contribution of albumin to redox processes. *Free Radic. Biol. Med.* **65**, 244–253
24. Turell, L., Botti, H., Carballal, S., Ferrer-Sueta, G., Souza, J. M., Durán, R., Freeman, B. A., Radi, R., and Alvarez, B. (2008) Reactivity of sulfenic acid in human serum albumin. *Biochemistry*. **47**, 358–367
25. Torres, M. J., Turell, L., Botti, H., Antmann, L., Carballal, S., Ferrer-Sueta, G., Radi, R., and Alvarez, B. (2012) Modulation of the reactivity of the thiol of human serum albumin and its sulfenic derivative by fatty acids. *Arch. Biochem. Biophys.* **521**, 102–110
26. Alvarez, B., Carballal, S., Turell, L., and Radi, R. (2010) Formation and reactions of sulfenic acid in human serum albumin. *Meth. Enzymol.* **473**, 117–136
27. Iversen, R., Andersen, P. A., Jensen, K. S., Winther, J. R., and Sigurskjold, B. W. (2010) Thiol-disulfide exchange between glutaredoxin and glutathione. *Biochemistry*. **49**, 810–820
28. Wood, J. L. (1987) Sulfane sulfur. *Meth. Enzymol.* **143**, 25–29
29. Carballal, S., Trujillo, M., Cuevasanta, E., Bartesaghi, S., Möller, M. N., Folkes, L. K., García-Bereguiaín, M. A., Gutiérrez-Merino, C., Wardman, P., Denicola, A., Radi, R., and Alvarez, B. (2011) Reactivity of hydrogen sulfide with peroxynitrite and other oxidants of biological interest. *Free Radic. Biol. Med.* **50**, 196–205
30. Park, C.-M., Macinkovic, I., Filipovic, M. R., and Xian, M. (2015) Use of the “tag-switch” method for the detection of protein S-sulhydration. *Meth. Enzymol.* **555**, 39–56
31. Saha, A., Goldstein, S., Cabelli, D., and Czapski, G. (1998) Determination of optimal conditions for synthesis of peroxynitrite by mixing acidified hydrogen peroxide with nitrite. *Free Radic. Biol. Med.* **24**, 653–9
32. Chai, J.-D., and Head-Gordon, M. (2008) Long-range corrected hybrid density functionals with damped atom-atom dispersion corrections. *Phys. Chem. Chem. Phys.* **10**, 6615–6620
33. Tomasi, J., Mennucci, B., and Cancès, E. (1999) The IEF version of the PCM solvation method: an overview of a new method addressed to study molecular solutes at the QM ab initio level. *J. Mol. Struct.: Theochem.* **464**, 211–226
34. Ditchfield, R., Hehre, W. J., and Pople, J. A. (1971) Self-consistent molecular-orbital methods. IX. An extended Gaussian-type basis for molecular-orbital studies of organic molecules. *J. Chem. Phys.* **54**, 724–728
35. Frisch, M. J., Trucks, G. W., Schlegel, H. B., Scuseria, G., Robb, M. A., Cheeseman, J. R., Scalmani, G., Barone, V., Mennucci, B., Petersson, G. A., Nakatsuji, H., Caricato, M., Li, X., Hratchian, H. P., Izmaylov, A. F., Bloino, J., Zheng, G., Sonnenberg, J. ., Hada, M., Ehara, M., Toyota, K., Fukuda, R., Hasegawa, J., Ishida, M., Nakajima, T., Honda, Y., Kitao, O., Nakai, H., Vreven, T., Montgomery, J. A., Peralta, J. E., Ogliaro, F., Bearpark, M., Heyd, J. J., Brothers, E., Kudin, K. N., Staroverov, V. N., Keith, T., Kobayashi, R., Normand, J., Raghavachari, K., Rendell, A., Burant, J. C., Iyengar, S. S., Tomasi, J., Cossi, M., Rega, N., Millam, J. M., Klene, M., Knox, J. E., Cross, J. B., Bakken, V., Adamo, C., Jaramillo, J., Gomperts, R., Stratmann, R. E., Yazyev, O., Austin, A. J., Cammi, R., Pomelli, C., Ochterski, J. W., Martin, R. L., Morokuma, K., Zakrzewski, V. G., Voth, G. A., Salvador, P., Dannenberg, J. J., Dapprich, S., Daniels, A. D., Farkas, O., Foresman, J. B., Ortiz, J. V., Cioslowski, J., and Fox, D. J. (2013) *Gaussian 09, Revision D.01 ed.*, Gaussian Inc.; Wallingford, CT
36. Bondi, A. (1964) van der Waals volumes and radii. *J. Phys. Chem.* **68**, 441–451
37. Fukui, K. (1981) The path of chemical reactions - the IRC approach. *Acc. Chem. Res.* **14**, 363–368
38. Hratchian, H. P., and Schlegel, H. B. (2005) Using Hessian updating to increase the efficiency of a Hessian based predictor-corrector reaction path following method. *J. Chem. Theory Comput.* **1**, 61–69
39. Geerlings, P., Fias, S., Boisdenghien, Z., and De Proft, F. (2014) Conceptual DFT: chemistry from the linear response function. *Chem. Soc. Rev.* **43**, 4989–5008
40. Yu, H.-Z., Yang, Y.-M., Zhang, L., Dang, Z.-M., and Hu, G.-H. (2014) Quantum-chemical predictions of pKa's of thiols in DMSO. *J. Phys. Chem. A.* **118**, 606–622
41. Mendes, P. (1993) GEPASI: a software package for modelling the dynamics, steady states and control of biochemical and other systems. *Comput. Appl. Biosci.* **9**, 563–71.

42. Liu, D. K., and Chang, S. G. (1987) Kinetic study of the reaction between cystine and sulfide in alkaline solutions. *Can. J. Chem.* **65**, 770–774
43. Singh, R., and Whitesides, G. M. (1993) Thiol—disulfide interchange. in *Sulphur-Containing Functional Groups (1993)*, pp. 633–658, John Wiley & Sons, Inc.
44. Vasas, A., Dóka, É., Fábrián, I., and Nagy, P. (2015) Kinetic and thermodynamic studies on the disulfide-bond reducing potential of hydrogen sulfide. *Nitric Oxide.* **46**, 93–101
45. Szajewski, R. P., and Whitesides, G. M. (1980) Rate constants and equilibrium constants for thiol-disulfide interchange reactions involving oxidized glutathione. *J. Am. Chem. Soc.* **102**, 2011–2026
46. Bunnett, J. F. (1963) Nucleophilic Reactivity. *Annu. Rev. Phys. Chem.* **14**, 271–290
47. Wilson, J. M., Bayer, R. J., and Hupe, D. J. (1977) Structure-reactivity correlations for the thiol-disulfide interchange reaction. *J. Am. Chem. Soc.* **99**, 7922–7926
48. Liu, C., Zhang, F., Munske, G., Zhang, H., and Xian, M. (2014) Isotope dilution mass spectrometry for the quantification of sulfane sulfurs. *Free Radic. Biol. Med.* **76**, 200–207
49. Asimakopoulou, A., Panopoulos, P., Chasapis, C. T., Coletta, C., Zhou, Z., Cirino, G., Giannis, A., Szabo, C., Spyroulias, G. A., and Papapetropoulos, A. (2013) Selectivity of commonly used pharmacological inhibitors for cystathionine β synthase (CBS) and cystathionine γ lyase (CSE). *Br. J. Pharmacol.* **169**, 922–932
50. Alvarez, B., Ferrer-Sueta, G., Freeman, B. A., and Radi, R. (1999) Kinetics of peroxynitrite reaction with amino acids and human serum albumin. *J. Biol. Chem.* **274**, 842–8
51. Frey, P. A., and Hegeman, A. D. (2007) *Enzymatic reaction mechanisms*, Oxford University Press, USA
52. Abiko, Y., Yoshida, E., Ishii, I., Fukuto, J. M., Akaike, T., and Kumagai, Y. (2015) Involvement of reactive persulfides in biological dimethylmercury sulfide formation. *Chem. Res. Toxicol.* **28**, 1301–1306
53. Cuevasanta, E., Denicola, A., Alvarez, B., and Möller, M. N. (2012) Solubility and permeation of hydrogen sulfide in lipid membranes. *PLoS ONE.* **7**, e34562
54. Mathai, J. C., Missner, A., Kugler, P., Saparov, S. M., Zeidel, M. L., Lee, J. K., and Pohl, P. (2009) No facilitator required for membrane transport of hydrogen sulfide. *Proc. Natl. Acad. Sci. U S A.* **106**, 16633–8
55. Vitvitsky, V., Yadav, P. K., Kurthen, A., and Banerjee, R. (2015) Sulfide oxidation by a noncanonical pathway in red blood cells generates thiosulfate and polysulfides. *J. Biol. Chem.* **290**, 8310–8320
56. Lagoutte, E., Mimoun, S., Andriamihaja, M., Chaumontet, C., Blachier, F., and Bouillaud, F. (2010) Oxidation of hydrogen sulfide remains a priority in mammalian cells and causes reverse electron transfer in colonocytes. *Biochim. Biophys. Acta.* **1797**, 1500–1511
57. Mishanina, T. V., Libiad, M., and Banerjee, R. (2015) Biogenesis of reactive sulfur species for signaling by hydrogen sulfide oxidation pathways. *Nat. Chem. Biol.* **11**, 457–464
58. Jackson, M. R., Melideo, S. L., and Jorns, M. S. (2012) Human sulfide:quinone oxidoreductase catalyzes the first step in hydrogen sulfide metabolism and produces a sulfane sulfur metabolite. *Biochemistry.* **51**, 6804–6815
59. Libiad, M., Yadav, P. K., Vitvitsky, V., Martinov, M., and Banerjee, R. (2014) Organization of the human mitochondrial hydrogen sulfide oxidation pathway. *J. Biol. Chem.* **289**, 30901–30910
60. Ono, K., Akaike, T., Sawa, T., Kumagai, Y., Wink, D. A., Tantillo, D. J., Hobbs, A. J., Nagy, P., Xian, M., Lin, J., and Fukuto, J. M. (2014) Redox chemistry and chemical biology of H₂S, hydropersulfides, and derived species: implications of their possible biological activity and utility. *Free Radic. Biol. Med.* **77**, 82–94
61. Creighton, T. E. (1975) Interactions between cysteine residues as probes of protein conformation: the disulfide bond between Cys-14 and Cys-38 of the pancreatic trypsin inhibitor. *J. Mol. Biol.* **96**, 767–776
62. Whitesides, G. M., Lilburn, J. E., and Szajewski, R. P. (1977) Rates of thiol-disulfide interchange reactions between mono- and dithiols and Ellman's reagent. *J. Org. Chem.* **42**, 332–338

63. Keire, D. A., Strauss, E., Guo, W., Noszal, B., and Rabenstein, D. L. (1992) Kinetics and equilibria of thiol/disulfide interchange reactions of selected biological thiols and related molecules with oxidized glutathione. *J. Org. Chem.* **57**, 123–127
64. Portillo-Ledesma, S., Sardi, F., Manta, B., Tourn, M. V., Clippe, A., Knoops, B., Alvarez, B., Coitino, E. L., and Ferrer-Sueta, G. (2014) Deconstructing the catalytic efficiency of peroxiredoxin-5 peroxidatic cysteine. *Biochemistry* **53**, 6113-6125.

FOOTNOTES

[†] This work was financed by grants from CSIC (Universidad de la República), and L'Oréal–UNESCO, Uruguay (to B.A.). E.C. and J.B. were supported by fellowships from the Agencia Nacional de Investigación e Innovación and by PEDECIBA, Uruguay. M.L. and M.R.F. acknowledge the support from the Emerging Field Initiative intramural grant from FAU Erlangen-Nuremberg (MRIC).

^a The mixture of H_2S and HS^- present in aqueous solution according to the working pH is referred as ' H_2S ', unless otherwise specified. The IUPAC-recommended names are sulfane and hydrogen sulfide for H_2S , and sulfanide and hydrogen(sulfide)(1-) for hydrosulfide anion, HS^- .

^b The term 'persulfides' is used in this text for the mixture of RSSH (hydrodisulfide derivative) and RSS^- (disulfanidyl derivative) in solution according to the working pH, unless otherwise specified. The IUPAC-recommended names for RSSH are disulfanyl and dithiohydroperoxide.

^c The abbreviations used are: HSA, human serum albumin; LMW, low molecular weight; DTNB, 5,5'-dithiobis-(2-nitrobenzoic acid); dtpa, diethylenetriaminepentaacetic acid; TNB, 5-thio-2-nitrobenzoic acid; GSSG, glutathione disulfide; GSH, glutathione; Cys-Cys, cysteine disulfide; Cys, cysteine; CysOMe-CysOMe, cystinedimethylester; CysOMe, cysteinemethylester; HED, hydroxyethylidysulfide; β -ME, β -mercaptoethanol; Hcy-Hcy, homocystine; Hcy, homocysteine; DTDPy, 4,4'-dithiodipyridine; DTT, dithiothreitol; TDMSP, tris(2,4-dimethyl-5-sulfophenyl)phosphine.

FIGURE LEGENDS

Figure 1. Kinetics of hydrogen sulfide consumption in the presence of glutathione disulfide. **A)** Na₂S (250 μM) was mixed with 2.0, 5.25 and 10.5 mM GSSG in phosphate buffer (100 mM, pH 7.4, 0.1 mM dtpa, 25 °C), in closed vials. Aliquots were analyzed for H₂S content with the methylene blue method. **B)** Observed rate constants for the reaction of HS⁻ with GSSG obtained from the fitting of time courses to single exponential equations.

Figure 2. Kinetics of reaction of hydrogen sulfide with HSA mixed disulfides. **A)** Na₂S (476 μM) was incubated with HSA-Cys (470 μM, black circles). Controls were prepared using Na₂S alone (476 μM, red squares) or Na₂S (118 μM) with HSA-SH (439 μM, blue diamonds) in tris buffer (0.2 M, pH 7.4, 0.1 mM dtpa, 25 °C). Aliquots were analyzed for H₂S content with the methylene blue method. **B)** Kinetics of H₂S decay in the presence of HSA-TNB, measured by selective H₂S electrode. Inset: original traces of H₂S decay upon addition of 34.5 μM (black line), 51.7 μM (red line), 172.4 μM (green line) and 344.7 μM (blue line) HSA-TNB into 10 μM Na₂S in phosphate buffer (50 mM, pH 7.4, 25 °C).

Figure 3. Comparison of the reactivities of HS⁻ and thiolates toward disulfides depending on the pK_a of the leaving thiol. **A)** pH-independent rate constants for the reactions of LMW disulfides with HS⁻ (this work) or with LMW thiolates (data reported in (45, 61, 47, 62)). **B)** pH-independent rate constants of the reactions of HS⁻ with mixed HSA disulfides.

Figure 4. Computational modeling of the reaction of hydrosulfide toward cystine. DFT optimized structures in water of the reactant complex, transition state and product complex for the reaction between cystine and HS⁻. Values in parentheses correspond to relative Gibbs free-energies at 298 K calculated respect to RC.

Figure 5. Comparison of the reactivities of HS⁻ and thiolates toward disulfides depending on the pK_a of the attacking thiol. **A) DTNB as electrophile.** pH-independent rate constants for the reactions of HS⁻ (this work) or thiolates (45, 47, 62) with DTNB. Data are grouped for thiocarboxyls (green squares), aryl thiols (red circles), alkyl thiols (blue triangles) and H₂S (black circle). Slopes (β_{nuc}) are 0.30, 0.38 and 0.46 for attacking thiocarboxyles, thioaryles and thioalkyls, respectively. **B) GSSG as electrophile.** pH-independent rate constants for alkyl thiols (blue triangles, (45, 61, 63)) and H₂S (black circle, this work).

Figure 6. KS-HOMO energies for thiolates, HS⁻ and CysSS⁻ calculated at the IEFPCM/ωB97X-D/6-31+G(d) level of theory as a function of pK_a of conjugated acid.

Figure 7. Product characterization. **A) Detection of sulfane sulfur.** HSA-Hcy (350 μM) was incubated with Na₂S (350 μM) during 3 hours. The reaction mixture was gel-filtrated using a PD-10 column and sulfanes were quantified in elution fractions by cold cyanolysis. **B) Dot-blot detection of HSA-SSH using the tag-switch assay.** Different mixed disulfides of HSA were treated with Na₂S to produce persulfides which were then labeled by tag-switch method. Duplicates of aliquots (5 μL) from the samples (30 μM) were added to a nitrocellulose membrane and the presence of biotinylation was visualized on radiographic films using chemiluminescent reagents.

Figure 8. Detection of HSA persulfide with tris(2,4-dimethyl-5-sulfohenyl)phosphine (TDMSP). **A-B)** Mass spectrum of the reaction mixture obtained by mixing HSA-SSH (20 μM) with TDMSP (400 μM) during 30 min at 25 °C. Two different *m/z* ranges are shown from the same spectrum, *m/z* 200-500 (A) and *m/z* 500-800 (B). The peak assignment (C-F) reveals that the most intense peaks correspond to unreacted TDMSP flying in cluster with one or two sodium cations (C-D). However, formation of TDMSP sulfide (TDMSP=S) could also be detected (E-F). Observed peaks (in blue) match perfectly the predicted isotopic distribution (in red). For TDMSP, the observed and predicted masses are 303.0111 and 303.0109, respectively, for the monosodium species, while the corresponding values for the disodium species are 629.0111 and 629.0116. For TDMSP=S, the

observed and predicted masses are 318.9972 and 318.9970, respectively, for the monosodium, or 660.9831 and 660.9837 for the disodium species.

Figure 9. Mass spectrometry of HSA persulfide. **A)** Mass spectrum of HSA-TNB (black) and HSA-TNB mixed with equimolar amounts of Na₂S (red). **B)** Zoomed overlay of the MS spectra showing difference. **C)** Deconvoluted mass spectra of HSA-TNB (black) and HSA-TNB + Na₂S (red). The spectrum shows the mass difference of 166 ± 1 suggesting the formation of protein persulfide. In addition, a peak assigned to HSA-SSO₃H could be also observed. **D)** Methodological approach to label and elute the peptide containing persulfidated cysteine. **E)** Observed (black) and simulated isotopic pattern of a peptide eluted following the protocol depicted in D). The mass is consistent with the doubly charged ALVLIAFAQYLQQ³⁴CPFEDHVK peptide. **F)** MS/MS spectrum confirms the sequence.

Figure 10. Competition kinetics for the reaction of HSA sulfenic acid with hydrogen sulfide. HSA-SOH (0.5 μM) was incubated with TNB (66 μM) and increasing concentrations of Na₂S in phosphate buffer (0.1 M, pH 7.4, 0.1 mM dtpa, 25 °C). **A)** Time course of TNB consumption at 412 nm. **B)** Correlation of k_{obs} versus concentration of Na₂S.

Figure 11. Effect of H₂O₂ on protein persulfidation in SH-SY5Y and HUVEC cells. **A)** SH-SY5Y cells were preincubated or not with 2 mM oxamic acid (OXA, inhibitor of cystathionine β-synthase and cystathionine γ-lyase) and treated with 300 μM H₂O₂ for 30 min. Cells were fixed with methanol and labeled for persulfide detection using the tag-switch assay. The biotinylation of the proteins was visualized by fluorescence microscopy using Dylight 488 streptavidin. Nuclei were stained with DAPI. **B)** The change in the fluorescence was semi-quantified using ImageJ, n = 100 from the experiment done in triplicates. Columns represent the mean ± S.E.M. * p < 0.01 versus control by analysis of variance (simple paired student's t-test). **C)** HUVEC were preincubated or not with 2 mM propargylglycine (PG, inhibitor of cystathionine γ-lyase) for 1.5 h and treated with 500 μM H₂O₂ for 30 min. Cells were fixed, labeled and visualized as in A). **D)** The change in the fluorescence was semi-quantified using ImageJ, n = 20 from the experiment done in triplicates. Columns represent the mean ± S.E.M. * p < 0.05 versus control or ** p = 0.053 versus H₂O₂ by analysis of variance (simple paired student's t-test).

Figure 12. Kinetics of the reaction of HSA persulfide with peroxyntirite. **A)** Kinetic traces of peroxyntirite decay (9 μM) in the presence of 7 (red), 20 (blue) and 40 μM (black) HSA-SSH. **B)** Analysis of kinetic traces using an initial rate approach for HSA-SSH (red diamonds) and HSA-SH (black squares). Error bars represent the standard deviation (n = 5).

Figure 13. Kinetics of the reaction of HSA persulfide with DTDPy. **A)** Kinetic traces of thiopyridone formation at 324 nm during the incubation of ~ 3 μM HSA-SSH (red) with 32 μM DTDPy are compared with those produced by 18 μM HSA-SH (black) and 3 μM HSA-SOH (blue) preparations. **B)** Dependence of k_{obs} on the concentration of DTDPy for HSA-SSH (red diamonds), HSA-SH (black squares) and HSA-SOH (blue triangles) preparations. **C)** Kinetic traces when HSA-SOH (6 μM, initial) was incubated with Na₂S (6 μM, initial) during 50 seconds and mixed with 32 μM DTDPy every 3 minutes. **D)** Red points: amplitudes obtained from fits of the first phase produced by incubation of DTDPy (32–207 μM) with the mixture of HSA-SOH and Na₂S (final concentration: 3 μM each) at different incubation times. Black line: numerical determination of the second-order rate constant between HSA-SOH and H₂S. The spontaneous decay of HSA-SOH was also considered. Rate constant estimated: $(4.7 \pm 0.2) \times 10^2 \text{ M}^{-1} \text{ s}^{-1}$.

TABLES

Table 1. Second-order rate constants for the reaction of hydrogen sulfide with symmetric LMW disulfides in 100 mM phosphate buffer at 25 °C.



Disulfide	p <i>K</i> _a of the thiol	<i>k</i> pH 7.4 (M ⁻¹ s ⁻¹)	<i>k</i> pH-indep (M ⁻¹ s ⁻¹)
DTNB	4.4 ^a	(8.61 ± 0.04) x 10 ²	(1.20 ± 0.01) x 10 ³
CysOMe-CysOMe	6.45 ^b	3.3 ± 0.7	5 ± 1
Cys-Cys	8.29 ^c	(6 ± 1) x 10 ⁻¹	(9 ± 2) x 10 ⁻¹
GSSG	8.94 ^c	(1.6 ± 0.1) x 10 ⁻¹	(2.2 ± 0.1) x 10 ⁻¹
Hcy-Hcy	9.1 ^c	(3.2 ± 0.4) x 10 ⁻¹	(4.5 ± 0.6) x 10 ⁻¹
HED	9.6 ^c	(3.92 ± 0.03) x 10 ⁻²	(5.48 ± 0.04) x 10 ⁻²

^aData from (25). ^bThe p*K*_a of CysOMe was determined by UV titration as in ref (64). ^cData from (64).

Table 2. Second-order rate constants for the reaction of hydrogen sulfide toward mixed disulfides formed between Cys34 of HSA and LMW thiols in 100 mM phosphate buffer at 25 °C.



Disulfide	$\text{p}K_a$ of the thiol	k pH 7.4 ($\text{M}^{-1} \text{s}^{-1}$)	k pH-indep ($\text{M}^{-1} \text{s}^{-1}$)
HSA-TNB	4.4 ^a	$(3.5 \pm 0.8) \times 10^2$	$(5 \pm 1) \times 10^2$
HSA-CysOMe	6.45 ^b	$(5.5 \pm 1.3) \times 10^1$	$(8 \pm 2) \times 10^1$
HSA-Cys	8.29 ^c	3.0 ± 1.1	4 ± 2
HSA-GSH	8.94 ^c	1.7 ± 1.1	2 ± 1
HSA-Hcy	9.1 ^c	$(2.3 \pm 0.8) \times 10^{-1}$	$(3 \pm 1) \times 10^{-1}$
HSA- β ME	9.6 ^c	$(5.1 \pm 0.4) \times 10^{-1}$	$(7.2 \pm 0.6) \times 10^{-1}$

^aData from (25). ^bThe $\text{p}K_a$ of CysOMe was determined by UV titration as in ref (64). ^cData from (64).

Table 3. Comparison of basicity, nucleophilicity (KS-HOMO energies) and chemical hardness (η) values for thiolates, HS⁻ and CysSS⁻ calculated at the DFT level in aqueous solution.

Species	p <i>K</i> _a	<i>E</i> _{HOMO} (eV)	η (eV)
CysOMe ⁻	6.45 ^a	-7.63	4.53
HS ⁻	7.00 ^b	-7.84	4.94
CysGly ⁻	7.95 ^c	-7.57	4.67
Cys ⁻	8.29 ^c	-7.50	4.72
Hcy ⁻	9.1 ^c	-7.33	4.58
β -ME ⁻	9.60 ^c	-7.39	4.75
CysSS ⁻	(4.34) ^d	-6.97	4.16

^aThis work. ^bData from (2). ^cData from (64). ^dEstimated here from the predicted shift respect to Cys of -3.96 (Eq. 3).

Figure 1

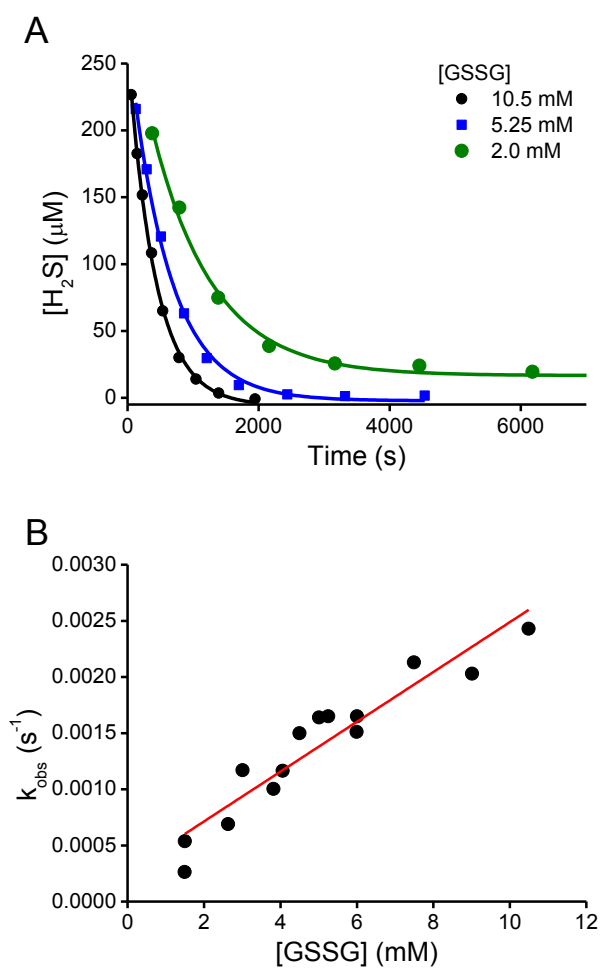


Figure 2

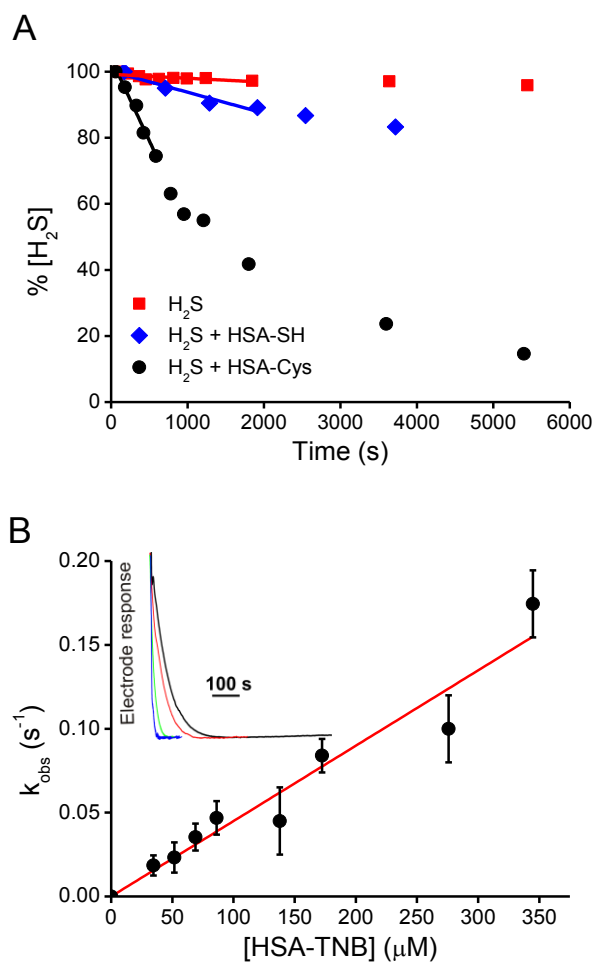


Figure 3

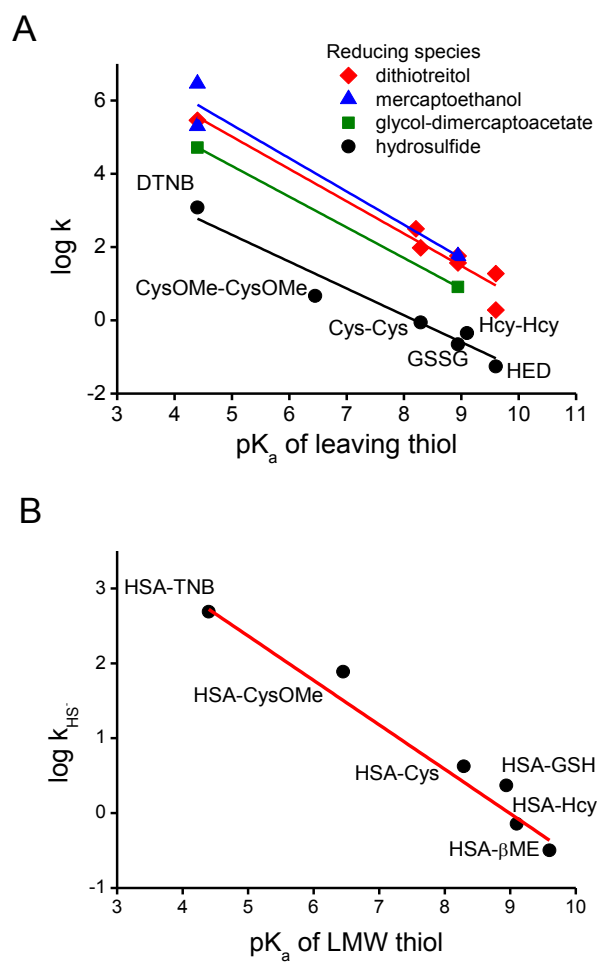


Figure 4

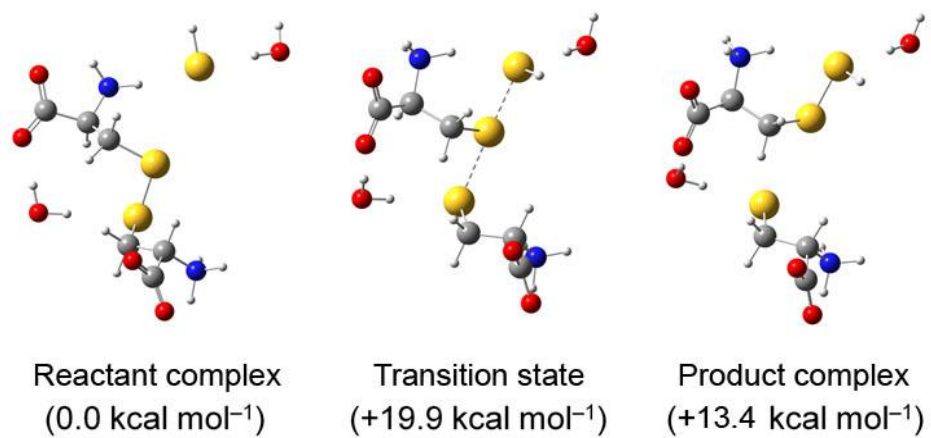


Figure 5

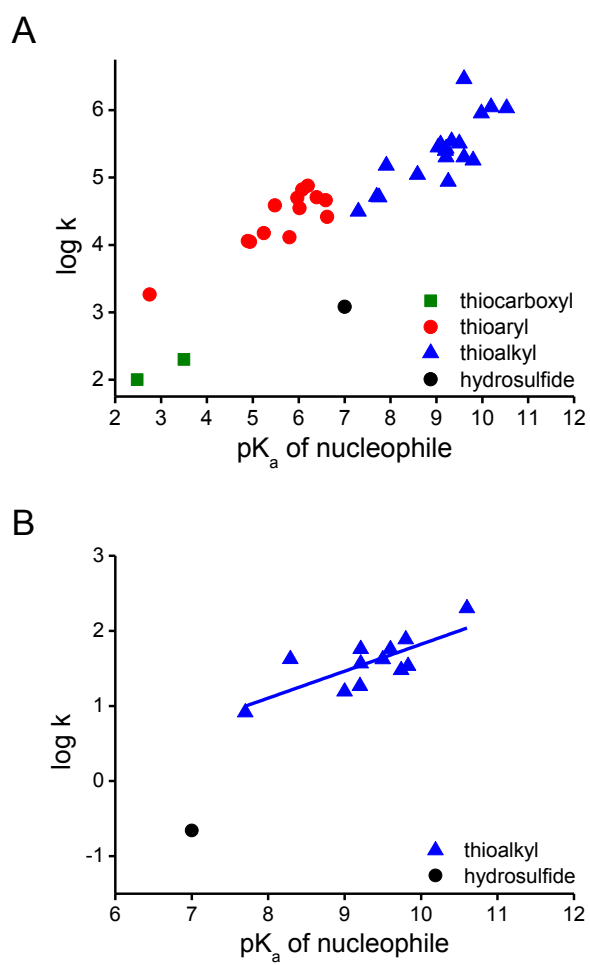


Figure 6

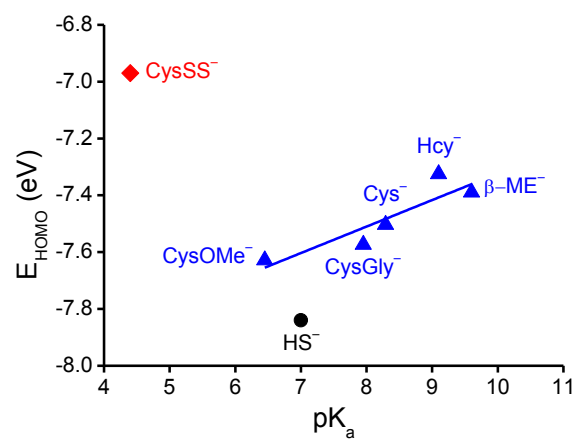


Figure 7

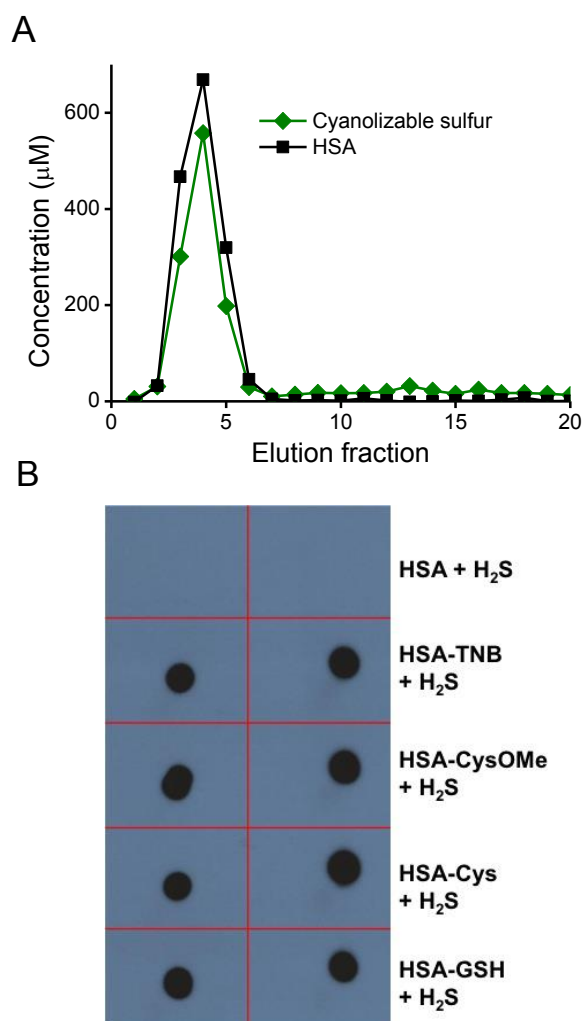


Figure 8

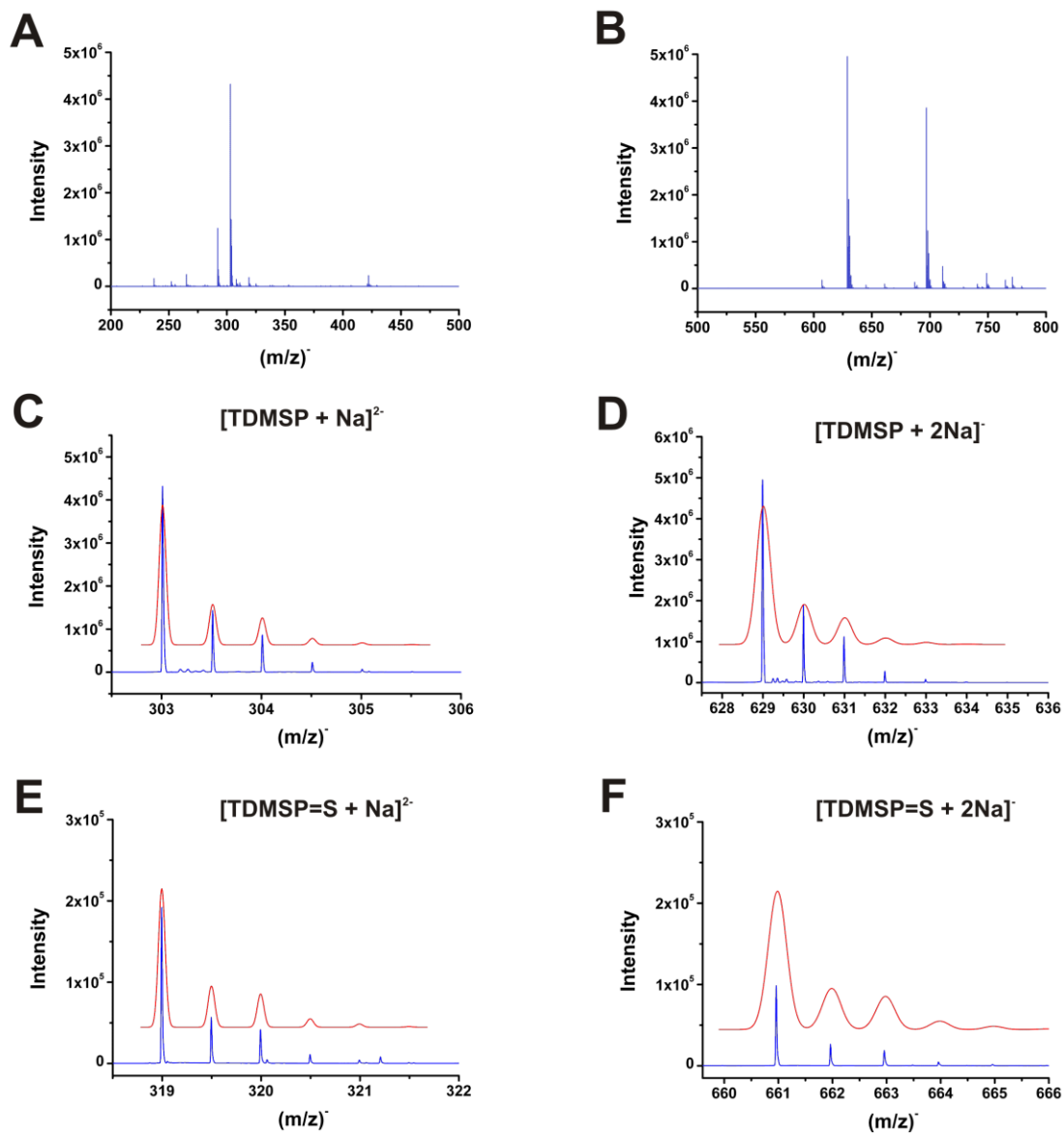


Figure 9

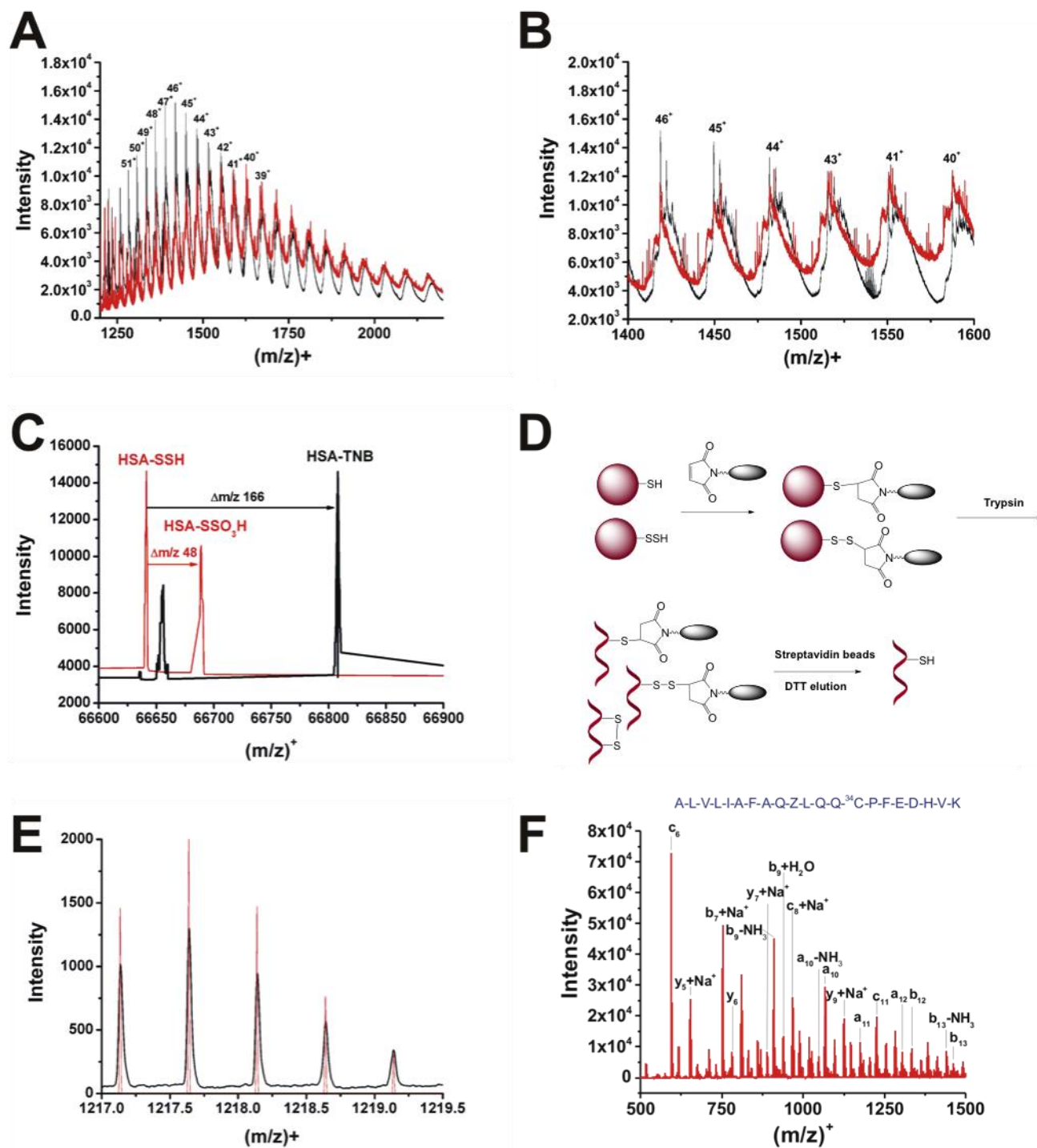


Figure 10

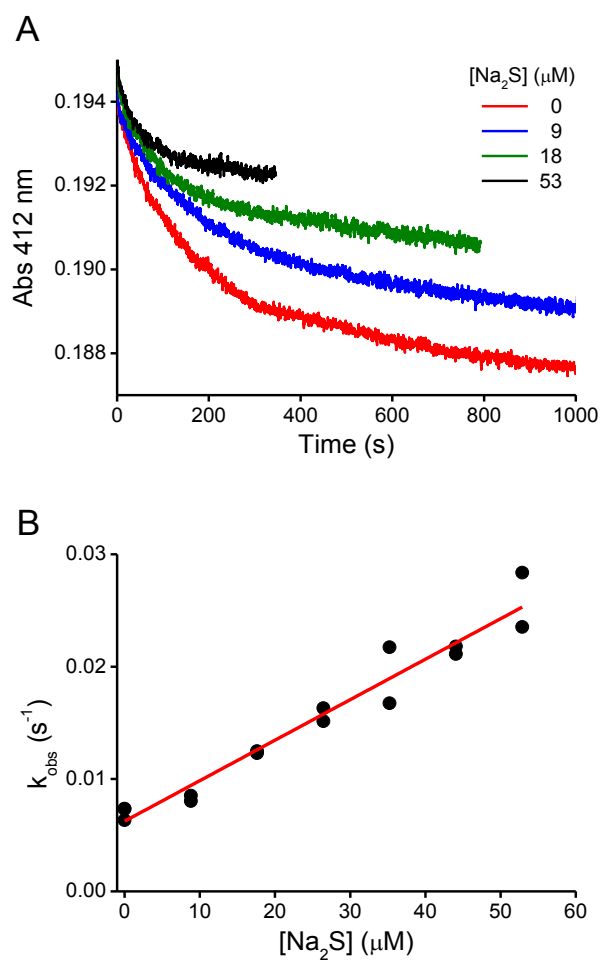


Figure 11

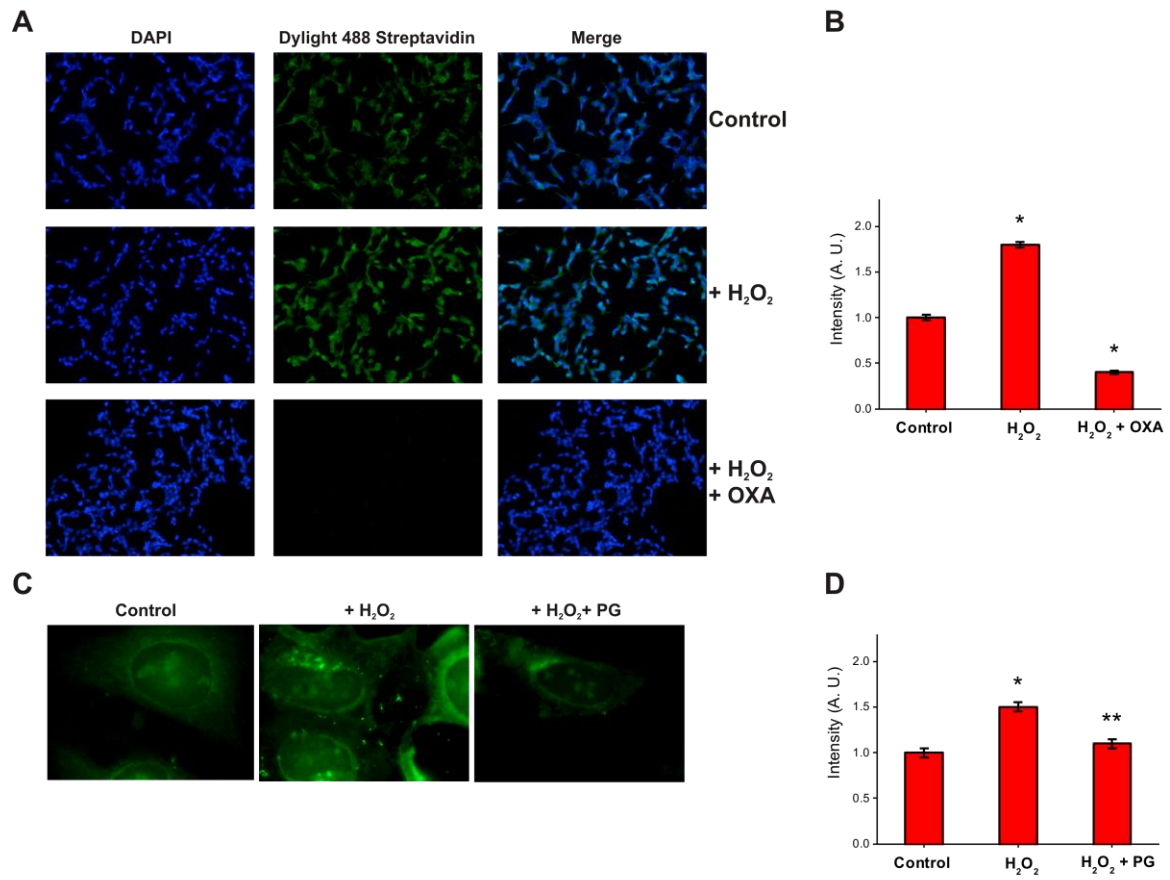
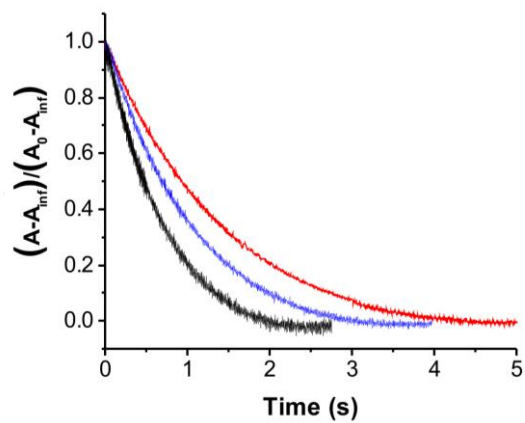


Figure 12

A



B

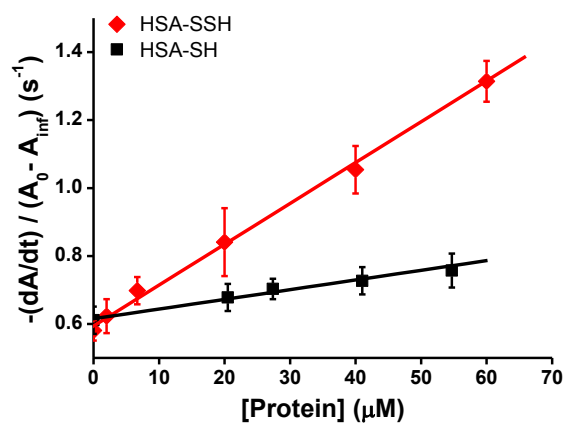
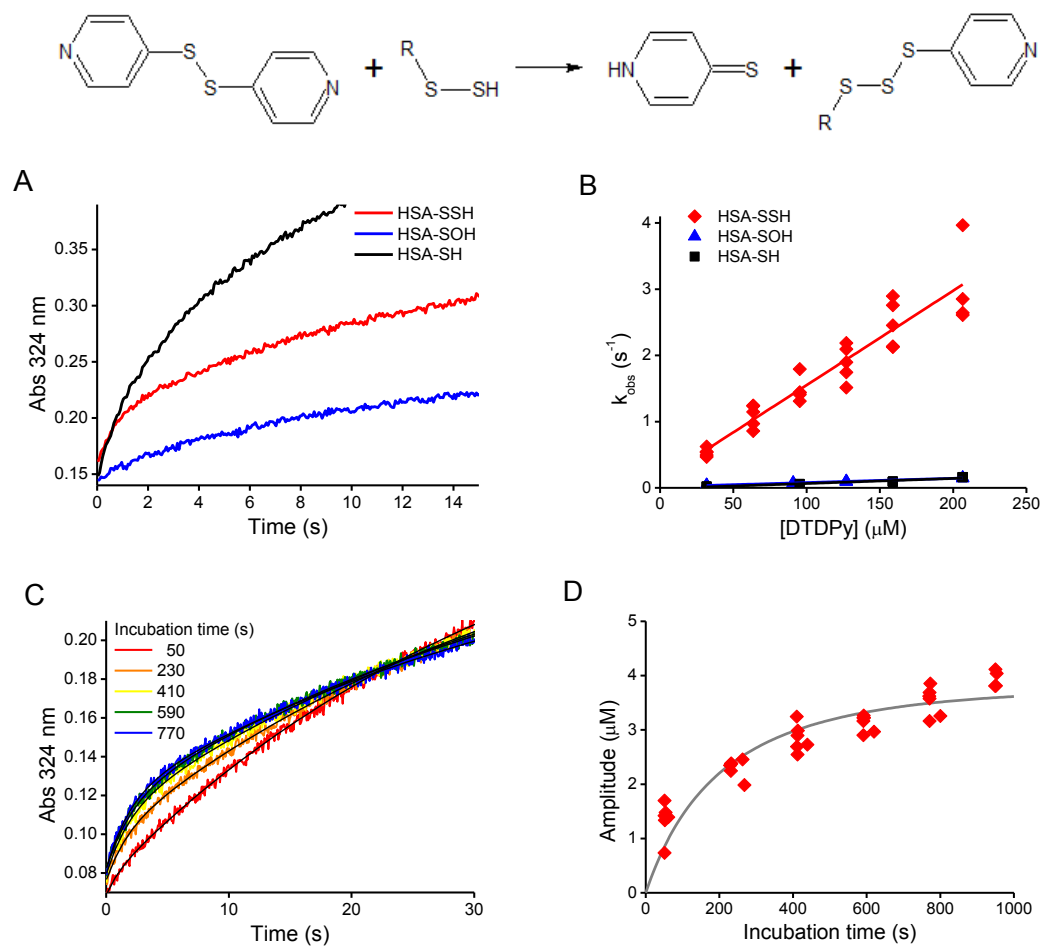


Figure 13



Enzymology:

Reaction of hydrogen sulfide with disulfide and sulfenic acid to form the strongly nucleophilic persulfide

Ernesto Cuevasanta, Mike Lange, Jenner Bonanata, E. Laura Coitiño, Gerardo Ferrer-Sueta, Milos R. Filipovic and Beatriz Alvarez
J. Biol. Chem. published online August 12, 2015



Access the most updated version of this article at doi: [10.1074/jbc.M115.672816](https://doi.org/10.1074/jbc.M115.672816)

Find articles, minireviews, Reflections and Classics on similar topics on the [JBC Affinity Sites](#).

Alerts:

- [When this article is cited](#)
- [When a correction for this article is posted](#)

[Click here](#) to choose from all of JBC's e-mail alerts

This article cites 0 references, 0 of which can be accessed free at <http://www.jbc.org/content/early/2015/08/12/jbc.M115.672816.full.html#ref-list-1>